Potential energy, Λ doubling and Born–Oppenheimer breakdown functions for the $B\,^1\Pi_u$ "barrier" state of Li_2

Yiye Huang and Robert J. Le Roy
Guelph-Waterloo Centre for Graduate Work in Chemistry, University of Waterloo, Waterloo, Ontario, Canada N2L 3G1

(Received 9 June 2003; accepted 17 July 2003)

The potential energy curve for the $B\,^1\Pi_u$ state of Li_2 has a rotationless barrier which protrudes above its energy asymptote. A direct fit to spectroscopic data for all three isotopomers of this species, including Λ-doubling splittings and tunneling predissociation line widths, is used to determine an accurate analytic potential energy function plus Born–Oppenheimer breakdown and Λ-doubling perturbation radial strength functions for this system. This analysis introduces an analytic model for representing a potential function with a rotationless barrier, and shows that a radial perturbation function treatment can determine the symmetry of the perturbing state giving rise to Λ-doubling splittings. © *2003 American Institute of Physics.* [DOI: 10.1063/1.1607313]

I. INTRODUCTION

It has becoming increasingly common to analyze diatomic molecule spectroscopic data by comparing observed transition energies with eigenvalue differences calculated numerically from an effective radial Schrödinger equation for a parametrized potential energy function and to use a least-squares fit to optimize the values of those potential function parameters.[1–12] Led by the pioneering work of Coxon and co-workers,[4,6,9,13–18] this approach has also come to be used routinely for determining the atomic-mass-dependent Born–Oppenheimer breakdown (BOB) functions which contribute to the overall electronic and centrifugal potential energy functions, terms which become particularly important when data for more than one isotopomer are being considered simultaneously.[5,8,10,19] For a wide variety of cases, this approach has been shown to represent the experimental data with equivalent accuracy and usually much more compactly than do conventional analyses based on fits to empirical level energy expressions. Unfortunately, the significance and practical utility of the potential energy and BOB functions determined in this way have often been undermined by shortcomings of the functional forms used to represent them. A means of addressing those problems for the BOB functions has recently been presented.[20] The present work examines problems associated with representing potential energy functions and determines an improved potential energy function for the $B\,^1\Pi_u$ state of Li_2 and the first BOB functions obtained for any state of Li_2.

One of the main problems encountered in using flexible analytic functions to represent diatomic molecule potential energy curves is their sometimes dubious extrapolation behavior outside the range of distances associated with the data used in the analysis. This may seem somewhat surprising, since the most widely used potential forms[8,11,15,21] are based on generalizations of the simple Morse potential, $V_M(r) = \mathcal{D}_e[1-e^{-\beta(r-r_e)}]^2$, and one might have expected that the algebraic structure of such functions would automatically impose realistic extrapolation behavior. However, the extrapolation behavior of the fitted exponent coefficient function $\beta=\beta(r)$ frequently led to physically absurd spurious potential minima or potential function turnover in the short-range region.[21–23] Fortunately, we have found that a judicious choice of the expansion variable used to define the radial dependence of such functions resolves most of those problems.[20,23] This method, together with an additional technique for addressing such problems in more difficult cases, is applied in the present study of the $B\,^1\Pi_u$ state of Li_2.

A second problem encountered in direct-potential-fit (DPF) analyses is the fact that none of the widely used Morse-type analytic functions can readily describe potentials with (rotationless) barriers which protrude above the potential asymptote. An analytic potential form which resolves this problem and also allows multiterm expressions for the long-range tail of the potential to be readily incorporated into a flexible general potential function is introduced here. This potential form and techniques for improving the extrapolation behavior of related analytic potential functions are presented in Sec. III. It is also shown that the effect of the perturbation giving rise to Λ-doubling level splittings can be represented efficiently and accurately by a distance-dependent coupling strength function incorporated as a potential energy correction term in the radial Schrödinger equation.

Another subject addressed here concerns the fact that although tunneling-predissociation level widths are strongly dependent on the details of the potential energy function, such data have not previously been used quantitatively in the determination of potential curves. The wealth of data of this type recently reported[24,25] for B-state Li_2 make it an ideal system for pursuing this possibility. Efficient and accurate methods for locating such metastable levels and calculating their tunneling widths and for utilizing such observations in data-analysis fits are presented in Sec. II, together with brief

descriptions of the underlying theory and of the computational methods used in the present analysis.

Finally, previously reported transition frequency[24,26,27] and tunneling predissociation level-width data[24,25] for $^{7,7}Li_2$ and $^{6,6}Li_2$ are combined with new transition frequency data for the two minor isotopomers[28] and used to determine an accurate analytical potential energy function and empirical BOB and Λ-doubling radial strength functions for this system. An overview of previous work on this system, a description of the data used, and the results of the present analysis are then presented in Sec. IV. A critical comparison of the analytical potential obtained here with the pointwise potential recently determined for this species from an analogous quantum-mechanical direct-fit analysis of the f-parity levels of the $^{7,7}Li_2$ isotopomer[27] then serves to illuminate the relative strengths of the two different approaches (analytic versus pointwise) for representing the potential energy function.

II. THEORY AND COMPUTATIONAL METHODS

As in most direct-potential-fit diatomic data analyses reported to date, the present approach starts from the effective radial Schrödinger equation derived by Watson,[29,30] in which nonadiabatic corrections to the kinetic energy operator are incorporated both into the atomic-mass-dependent "adiabatic" BOB contribution to the electronic potential energy function and into the nonadiabatic BOB contribution to the effective centrifugal potential of the rotating molecule. Following the convention of Ref. 32, the resulting radial Schrödinger equation for isotopomer-α of species $A-B$ in a $^1\Sigma$ state may be written as

$$\left\{ -\frac{\hbar^2}{2\mu_\alpha}\frac{d^2}{dr^2} + [V_{\rm ad}^{(1)}(r) + \Delta V_{\rm ad}^{(\alpha)}(r)] + \frac{\hbar^2 J(J+1)}{2\mu_\alpha r^2}[1+g^{(\alpha)}(r)] \right\} \psi_{v,J}(r) = E_{v,J}\psi_{v,J}(r), \quad (1)$$

where μ_α is the reduced mass of atoms A and B with atomic masses $M_A^{(\alpha)}$ and $M_B^{(\alpha)}$, $V_{\rm ad}^{(1)}(r)$ is the total internuclear potential for the selected reference isotopomer (labeled $\alpha=1$), $\Delta V_{\rm ad}^{(\alpha)}(r)$ is the effective "adiabatic" BOB potential correction for isotopomer α, the *difference* between the effective adiabatic potentials for isotopomer-α and for the reference species ($\alpha=1$), and $g^{(\alpha)}(r)$ is the nonadiabatic contribution to the centrifugal potential for isotopomer-α. Both $\Delta V_{\rm ad}^{(\alpha)}(r)$ and $g^{(\alpha)}(r)$ are written as a sum of two terms, one for each component atom, whose magnitudes are inversely proportional to the mass of the particular atomic isotope,[29,31–33]

$$\Delta V_{\rm ad}^{(\alpha)}(r) = \frac{\Delta M_A^{(\alpha)}}{M_A^{(\alpha)}}\tilde{S}_{\rm ad}^A(r) + \frac{\Delta M_B^{(\alpha)}}{M_B^{(\alpha)}}\tilde{S}_{\rm ad}^B(r), \quad (2)$$

$$g^{(\alpha)}(r) = \frac{M_A^{(1)}}{M_A^{(\alpha)}}\tilde{R}_{\rm na}^A(r) + \frac{M_B^{(1)}}{M_B^{(\alpha)}}\tilde{R}_{\rm na}^B(r), \quad (3)$$

where $\Delta M_A^{(\alpha)} = M_A^{(\alpha)} - M_A^{(1)}$ and $\Delta M_B^{(\alpha)} = M_B^{(\alpha)} - M_B^{(1)}$ are the differences between the atomic masses in the isotopomer of interest and in the chosen reference isotopomer.[32]

A. Treatment of Λ doubling

For a non-Σ singlet state, the angular momentum factor $[J(J+1)]$ in Eq. (1) is replaced by $[J(J+1)-\Lambda^2]$ (or in Hund's case c, by $[J(J+1)-\Omega^2]$). In addition, interaction of the electronic orbital angular momentum with the rotational angular momentum gives rise to a splitting of the e- and f-parity components of the individual J levels, which increases with J.[34–36] This splitting can be attributed to a coupling to one or more nearby electronic states whose Λ values differ by 1 from that for the state of interest. For levels of a $^1\Pi$ state being perturbed by a $^1\Sigma$ state, the matrix element of this uncoupling operator between level v of the $^1\Pi$ state in question and level v' of the perturbing $^1\Sigma$ state is equal to $\langle \psi_{v,J}^{\Pi}(r) | \eta_{\rm el}(r)(\hbar^2/2\mu_\alpha r^2) | \psi_{v',J}^{\Sigma}(r) \rangle \sqrt{J(J+1)}$, where $\eta_{\rm el}(r)$ is a dimensionless electronic matrix element which varies slowly with r.[35,36] Within second-order perturbation theory, this gives rise to the level energy shift

$$\delta E_\Lambda(v,J) = [J(J+1)] \sum_{v'} \frac{\langle \psi_{v,J}^{\Pi}(r) | \frac{\eta_{\rm el}(r)\hbar^2}{2\mu_\alpha r^2} | \psi_{v',J}^{\Sigma}(r) \rangle \langle \psi_{v',J}^{\Sigma}(r) | \frac{\eta_{\rm el}(r)\hbar^2}{2\mu_\alpha r^2} | \psi_{v,J}^{\Pi}(r) \rangle}{E_{v,J}^{\Pi} - E_{v',J}^{\Sigma}}, \quad (4)$$

where the sum runs over all bound and continuum levels [denoted $v'=v'(^1\Sigma)$] of the perturbing $^1\Sigma$ state. For a $^1\Sigma^+$ perturbing state this interaction only couples to the e-parity levels of the $^1\Pi$ state, and for a $^1\Sigma^-$ state it only shifts the f sublevels.

If the levels of the perturbing state which make dominant contributions to the sum in Eq. (4) lie relatively close to one another and relatively far from the $v(^1\Pi)$ level of interest, an Ünsold-type approximation[37,38] allows Eq. (4) to be written as

$$\delta E_\Lambda(v,J) \approx \frac{\langle \psi_{v,J}^{\Pi}(r) | \left(\frac{\eta_{\rm el}(r)\hbar^2}{2\mu_\alpha r^2} \right)^2 | \psi_{v,J}^{\Pi}(r) \rangle}{E_{v,J}^{\Pi} - \overline{E}_J^{\Sigma}(v)} [J(J+1)] = {\rm sg}(e,f) q_1^{(\alpha)}(v) [J(J+1)], \quad (5)$$

where $\overline{E}_J^{\Sigma}(v)$ is an average energy for the $v'(^1\Sigma)$ levels making the dominant contributions to the sum in Eq. (4), and ${\rm sg}(e,f)$ is a dimensionless numerical factor which is defined

below. If one makes the additional approximations (i) that $\eta_{\rm el}(r)$ be replaced by the average value $\overline{\eta_{\rm el}(r)}=\sqrt{2}$, (ii) that the expectation value of $(\hbar^2/2\mu_\alpha r^2)^2$ equals the square of the expectation value of $(\hbar^2/2\mu_\alpha r^2)$,

$$\langle\psi^{\Pi}_{v,J}(r)|\left(\frac{\hbar^2}{2\mu_\alpha r^2}\right)^2|\psi^{\Pi}_{v,J}(r)\rangle \approx\langle\psi^{\Pi}_{v,J}(r)|\frac{\hbar^2}{2\mu_\alpha r^2}|\psi^{\Pi}_{v,J}(r)\rangle^2=[B_v(J)]^2, \tag{6}$$

where $B_v(J)\equiv\partial E_{v,J}/\partial[J(J+1)]$, and (iii) that the effect of centrifugal distortion on $B_v(J)$ can be neglected, one obtains the simplified expression for $q_1^{(\alpha)}(v)$ quoted by Herzberg[34] [his Eq. (V,27)]. Equation (5) is commonly used in cases in which the levels of the perturbing state do not lie too close to those of the $^1\Pi$ levels of interest.[34,39] Practical empirical analyses using this approach usually allow for multiple terms of the form $q_m^{(\alpha)}(v)[J(J+1)]^m$ and either determine the coefficients for each vibrational level of each isotopomer or represent them by empirical power series in $(v+\frac{1}{2})$. In either case, the vibrational dependence of the splitting constant is predicted to be roughly proportional to that of the square of the inertial rotational constant $B_v=B_v(J=0)$, which confirms[34] that in a combined-isotopomer treatment the Λ-doubling level shifts scale as $(\mu_\alpha)^{-2}$.

Equation (5) clearly has the form of a first-order perturbation theory energy correction. This suggests that one can express the magnitude and sign of the Λ-doubling perturbation in terms of an effective perturbation strength function

$$\Delta V_\Lambda^{(\alpha)}(r)=\left(\frac{\hbar^2}{2\mu_\alpha r^2}\right)^2 f_\Lambda(r), \tag{7}$$

where

$$f_\Lambda(r)=[\eta_{\rm el}(r)]^2/[E^{\Pi}_{v,J}-\overline{E}^{\Sigma}_J(v)] \tag{8}$$

has units $[\text{energy}]^{-1}$ and is expected to be only weakly dependent on r. Before proceeding further, however, we must delineate the sign convention associated with Λ-doubling level shifts and the definition of the $q_m^{(\alpha)}(v)$ constants.

The above discussion indicates that the algebraic sign of the energy correction is determined by the sign of the Ünsold energy difference $[E^{\Pi}_{v,J}-\overline{E}^{\Sigma}_J(v)]$. However, the established convention for $q_m^{(\alpha)}(v)$ coefficients is that their contribution to the level energy is $+q_m^{(\alpha)}(v)[J(J+1)]^m$ for e-parity levels and $-q_m^{(\alpha)}(v)[J(J+1)]^m$ for f-parity levels. The effective radial Schrödinger equation used in the present work therefore has the form

$$\left\{-\frac{\hbar^2}{2\mu_\alpha}\frac{d^2}{dr^2}+[V_{\rm ad}^{(1)}(r)+\Delta V_{\rm ad}^{(\alpha)}(r)] +\frac{\hbar^2}{2\mu_\alpha r^2}[J(J+1)-\Lambda^2][1+g^{(\alpha)}(r)] +{\rm sg}(e,f)\Delta V_\Lambda^{(\alpha)}(r)[J(J+1)]\right\}\psi_{v,J}(r)=E_{v,J}\psi_{v,J}(r). \tag{9}$$

If the dominant perturbing state has $^1\Sigma^+$ symmetry, ${\rm sg}(e,f)=+1$ for e-parity levels and $=0$ for f levels, while if it is a $^1\Sigma^-$ state, ${\rm sg}(e,f)=0$ for e-parity levels and $=-1$ for f levels. If the identity of the dominant perturbing state is not known or one does not wish to make any *a priori* assumptions about its properties, ${\rm sg}(e,f)$ is normally set equal to $+\frac{1}{2}$ for e-parity levels and $-\frac{1}{2}$ for f levels.

In summary, the present work takes account of Λ-doubling perturbations by addition of the potential energy term ${\rm sg}(e,f)\Delta V_\Lambda(r)[J(J+1)]$ to the radial Schrödinger equation. For the $B\,^1\Pi_u$ state of Li_2, all of the nearby $^1\Sigma$ states have $^1\Sigma^+$ symmetry,[40] so (unless stated otherwise) the present analysis defines ${\rm sg}(e,f)=+1$ for e-parity levels and $=0$ for f levels. The particular expressions used to represent the overall potential energy function $V_{\rm ad}^{(1)}(r)$, the atom-specific BOB functions $\Delta V_{\rm ad}^{\rm Li}(r)$ and $q_{\rm Li}(r)$, and the Λ-doubling radial strength function $f_\Lambda(r)$, are described in Secs. III and IV.

B. Tunneling predissociation linewidths

For an electronic state with a potential barrier which protrudes above the asymptote at distances larger than the potential minimum,[41] the molecule may predissociate by tunneling through that barrier, a process which slightly shifts those ''quasibound'' levels and broadens associated spectral lines. These tunneling predissociation linewidths are experimental observables which depend upon the potential energy function and hence can be included with the transition frequencies in the data set used to determine that interaction potential. However, to do so requires efficient and accurate methods for determining their energies and calculating their widths which can readily be incorporated into the data analysis procedure.

Strictly speaking, the energies and widths of quasibound levels observed in ''discrete'' spectra can only be predicted accurately by a detailed quantum-mechanical bound $\rightarrow$continuum simulation of the intensity profile associated with each transition into that ''level.'' However, that approach would be too cumbersome to incorporate into an automated least-squares data analysis procedure. Fortunately, efficient and accurate approximate methods for locating quasibound levels and calculating their widths were developed a number of years ago.[42–44] In particular, it was found that very accurate level energies could be obtained by combining the usual wave function boundary condition at $r\rightarrow 0$ with the requirement that at the outermost classical turning point $r_3(E_{v,J})$ associated with energy level $E_{v,J}$ (see Fig. 1), the wave function must behave like an Airy function of the second kind, $Bi(r_3(E_{v,J})-r)$.[45] This reduces the problem of locating such metastable levels to the same two-boundary-condition eigenvalue problem associated with truly bound levels, and allows application of the standard, rapidly convergent Numerov–Cooley predictor–corrector procedure.[46,47] Quasibound level energies obtained in this way agree with those yielded by the best alternate methods to within a few percent of the associated level width,[42,43] discrepancies smaller than those usually associated with experimental determination of such line positions. This method of

located quasibound levels is implemented in the widely used eigenvalue subroutine SCHRQ utilized in the present work.[48]

A simple physical description of tunneling predissociation considers the molecule in quasibound level (v,J) at total energy $E=E_{v,J}>\mathfrak{D}$ (where $\mathfrak{D}$ is the energy at the potential asymptote) as being trapped behind the potential barrier and vibrating in the well bounded by turning points $r_1(E_{v,J})$ and $r_2(E_{v,J})$ (see Fig. 1). The point mass μ collides with the barrier with a frequency of $[1/t_{\rm vib}(E_{v,J})]\ {\rm s}^{-1}$, where $t_{\rm vib}(E_{v,J})$ is the period of vibration for that level, and on each collision there is a finite probability $\kappa(E_{v,J})$ that quantum-mechanical tunneling will allow predissociation to occur.[49] As a result, the tunneling predissociation lifetime is $\tau_{\rm tp}=t_{\rm vib}(E_{v,J})/\kappa(E_{v,J})$ and the associated [full width at half maximum (FWHM)] level width is

$$\Gamma^{\rm tp}_{v,J}=\hbar/\tau_{\rm tp}=\hbar\,\kappa(E_{v,J})/t_{\rm vib}(E_{v,J}). \tag{10}$$

In a simple classical treatment,

$$t_{\rm vib}(E_{v,J})\approx t^{\rm cl}_{\rm vib}(E_{v,J})=\hbar\sqrt{\frac{2\mu}{\hbar^2}}\int_{r_1(E_{v,J})}^{r_2(E_{v,J})}[E_{v,J}-V(r)]^{-1/2}dr, \tag{11}$$

and the conventional first-order semiclassical treatment of barrier tunneling implies that[49,50]

$$\kappa(E_{v,J})\approx\kappa_{\rm sc}(E_{v,J})=e^{-\varepsilon(E_{v,J})}, \tag{12}$$

where

$$\varepsilon(E_{v,J})=2\sqrt{\frac{2\mu}{\hbar^2}}\int_{r_2(E_{v,J})}^{r_3(E_{v,J})}[V(r)-E_{v,J}]^{1/2}dr. \tag{13}$$

This formulation gives realistic estimates of level widths, particularly for long-lived levels lying well below the potential barrier maximum. However, its simple (semi)classical origin introduces unphysical artifacts, such as a singularity in $t^{\rm cl}_{\rm vib}(E_{v,J})$ and tunneling efficiency of 100% when $E_{v,J}$ lies precisely at the barrier maximum.

Fortunately, a uniform semiclassical treatment defined in terms of the same phase integrals of Eqs. (11) and (13) yields the much more accurate expressions[44]

$$\kappa_{\rm un}(E_{v,J})=4\left(\frac{[1+e^{-\varepsilon(E_{v,J})}]^{1/2}-1}{[1+e^{-\varepsilon(E_{v,J})}]^{1/2}+1}\right) \tag{14}$$

and[43,51]

$$t^{\rm un}_{\rm vib}(E_{v,J})=t^{\rm cl}_{\rm vib}(E_{v,J})-\frac{\hbar}{2\pi}\left[\ln\{\varepsilon(E_{v,J})/2\pi\}-2\pi\frac{d\mathcal{A}rg\Gamma(\frac{1}{2}-i\varepsilon(E_{v,J})/2\pi)}{d\varepsilon(E_{v,J})}\right]\frac{\partial\varepsilon(E_{v,J})}{\partial E_{v,J}}, \tag{15}$$

where $\Gamma(a+iy)$ is a gamma function of complex argument, and Eq. (6.1.27) of Ref. 45 shows that

$$\frac{dArg\Gamma(\frac{1}{2}-i\varepsilon(E_{v,J})/2\pi)}{d\varepsilon(E_{v,J})}=\Psi\left(\frac{1}{2}\right)+\sum_{k=0}1\Big/\left(k+\frac{1}{2}\right)\times\left\{\left[2\pi\left(k+\frac{1}{2}\right)\Big/\varepsilon(E_{v,J})\right]^2+1\right\}, \tag{16}$$

where Ψ is the digamma function and $\Psi(\frac{1}{2})=-1.96351\,00260\,21423\ldots$.[45] For a level lying precisely at the barrier maximum, the singularity in $t^{\rm cl}_{\rm vib}(E_{v,J})$ and the logarithmic term in Eq. (15) precisely cancel one another, and the resulting predicted level widths for energies very near the barrier maximum are quite reliable.

In summary, therefore, the recommended method for calculating the tunneling predissociation level width $\Gamma^{\rm tp}_{v,J}$ (or tunneling lifetime $\tau_{\rm tp}$) is to use Eq. (10), with $\kappa(E_{v,J})$ and $t_{\rm vib}(E_{v,J})$ calculated using Eqs. (14) and (15), respectively. Detailed numerical tests indicate that for levels lying below a potential barrier maximum, this approach yields results as accurate as can be obtained without performing a detailed numerical bound→continuum simulation of the particular transition being probed.[42–44] However, in view of this method's neglect of background phase shifts[44] and of possible errors associated with the precise determination of the energy $E_{v,J}$ at which $\kappa_{\rm un}(E_{v,J})$ and $t^{\rm un}_{\rm vib}(E_{v,J})$ are being evaluated, one should probably associate a computational uncertainty of a few percent (say, ca. 5%–10%) with level widths calculated in this way. As a result, the overall uncertainty used to define the weight of a given experimental width datum in a least-squares fit procedure should be the square root of the sum of the square of this 5%–10% uncertainty plus the square of the experimental uncertainty, which is also typically 5%–10% of the width. The net effect of taking proper account of this computational uncertainty is to slightly reduce the weight given to the width data in the fits. On the other hand, the alternative of performing a direct numerical bound-to-continuum simulation for each observation of a predissociating level and determining the associated partial derivatives by differences, would be unacceptably tedious for inclusion in an automated direct-potential-fit analysis, so this modest loss of influence is usually tolerable.

The closed-form expression for level widths obtained above greatly facilitates the inclusion of level width measurements in least-squares data analyses, since it allows the partial derivatives of the widths with respect to parameters of the potential $\{p_j\}$ to be computed directly, which is much more efficient and accurate than using numerical differentiation. In particular, straightforward application of the chain rule allows the required partial derivatives of $\Gamma^{\rm tp}_{v,J}$ to be expressed in terms of partial derivatives of the phase integrals $\varepsilon(E_{v,J})$ and $t^{\rm cl}_{\rm vib}(E_{v,J})$ and related terms. The phase integrals associated with the partial derivatives of $\varepsilon(E_{v,J})$,

$$\left.\frac{\partial\varepsilon(E_{v,J})}{\partial E_{v,J}}\right|_{\{p_j\}}=-\sqrt{\frac{2\mu}{\hbar^2}}\int_{r_2(v,J)}^{r_3(v,J)}[V(r)-E_{v,J}]^{-1/2}dr, \tag{17}$$

$$\left.\frac{\partial \varepsilon(E_{v,J})}{\partial p_i}\right|_{\{p_j;j\neq i\},E_{v,J}} = +\sqrt{\frac{2\mu}{\hbar^2}}\int_{r_2(v,J)}^{r_3(v,J)}\frac{\partial V(r)}{\partial p_i}[V(r)-E_{v,J}]^{-1/2}dr, \quad (18)$$

have the same type of integrable singularity at the turning points seen in Eq. (11) and can readily be evaluated by standard numerical methods (see, e.g., Sec. 25.4.38 of Ref. 45). However, the analogous partial derivatives of $t_{\rm vib}^{\rm cl}(E_{v,J})$ are not so standard, since differentiation of that integrand yields apparent nonintegrable singularities at the turning points.

Fortunately, methods for treating high-order phase integrals of this type were developed some years ago.[52,53] The most elegant and efficient of these is the one devised by Pajunen and co-workers,[52,54] in which line integrals of the type appearing in Eqs. (11), (17), and (18) are first written as contour integrals in the complex plane,

$$\mathrm{I}_k(\{f\}) = \tfrac{1}{2}\oint_{\Upsilon(r_a,r_b)} dr f(r) \Big/ |E_{v,J}-V(r)|^{k+1/2}, \quad (19)$$

where $\Upsilon(r_a,r_b)$ is a contour in the complex plane surrounding the segment of the real line running between the two turning points r_a and r_b, and $f(r)$ is some known function. In this notation $t_{\rm vib}^{\rm cl}(E_{v,J}) = \hbar\sqrt{2\mu/\hbar^2}\,\mathrm{I}_0^{\rm well}(\{1\})$ [where the superscript "well" refers to the fact that r_a and r_b are $r_1(E_{v,J})$ and $r_2(E_{v,J})$, respectively], and the general recurrence relations[55]

$$\partial \mathrm{I}_k^{\rm well}(\{f\})/\partial E_{v,J} = -\left(k+\frac{1}{2}\right)\mathrm{I}_{k+1}^{\rm well}(\{f\}), \quad (20)$$

$$\partial \mathrm{I}_k^{\rm well}(\{1\})/\partial p_j = +\left(k+\frac{1}{2}\right)\mathrm{I}_{k+1}^{\rm well}\left(\left\{\frac{\partial V(r)}{\partial p_j}-\frac{\partial E_{v,J}}{\partial p_j}\right\}\right) \quad (21)$$

allow the derivatives of $\mathrm{I}_0(\{f\})$ to be expressed in terms of $k=1$ contour integrals. Integrals of this type are readily evaluated using the Pajunen–Child method, in which the contour integral in the complex plane is evaluated using a straightforward Gaussian-like quadrature procedure involving a weighted sum of integrand values calculated at particular points on the real line. This approach allows the straightforward and accurate calculation of the partial derivatives required herein.[56]

C. Fitting procedure

The combined-isotopomer direct-potential-fit analysis of transition energy and level width data for the $B\,^1\Pi_u$ state of Li_2 reported below was performed using program DSPOTFIT.[56] In the fits, each experimental datum $y_{\rm obs}(i)$ is weighted by the inverse square of the associated estimated uncertainty $unc(i)$, and the overall quality of fit is indicated by the dimensionless root-mean-square residual (rmsr),

$$\mathrm{rmsr} = \left\{N^{-1}\sum_{i=1}^{N}\{[y_{\rm calc}(i)-y_{\rm obs}(i)]/unc(i)\}^2\right\}^{1/2}, \quad (22)$$

where $y_{\rm calc}(i)$ is the value of datum i calculated using the optimized set of parameters, and N is the total number of data. Values of rmsr$\lesssim$1 indicate that the fit has, on average, accounted for all of the data within their uncertainties. This measure of the quality of a fit is used in preference to the dimensionless standard error $\overline{\sigma}_f$ [defined by the same expression, but with the factor N^{-1} replaces by $(N-M)^{-1}$, where M is the number of free parameters] because it may readily be applied to separate subsets of data such as level widths, as well as to the overall fit.

The parameter uncertainties reported herein are 95% confidence limit uncertainties, and the reported parameters were determined using the sequential rounding and refitting procedure of Ref. 57 to yield accurate parameter values with a minimum number of required significant digits.

III. POTENTIAL ENERGY AND CORRECTION FUNCTIONS

A. Three types of potential energy function forms

In the earliest applications of the direct-potential fit (DPF) approach to diatomic molecule data analysis, the potential energy function was represented by what we call a "polynomial-corrected pointwise potential" (PCPP), a set of turning points determined from the first-order semiclassical RKR inversion procedure plus an analytic correction function represented by some set of basis functions, often orthogonal polynomials.[1–3] For systems with small reduced masses that approach yielded significant improvements over the accuracy of simple first-order RKR potentials. However, the resulting potential functions consist of large arrays of irregularly spaced turning points, which for practical use had to be quoted to many significant digits and interpolated over. Moreover, the polynomial-type correction functions used in most applications do not extrapolate in a realistic manner, so this approach provides no sensible description of the system beyond the range of distances spanned by the data used in the analysis. Thus, such potentials are at best inconvenient to import and use in other work, and in recent years this approach has been supplanted by others.

A more sophisticated type of pointwise potential has recently been introduced by Pashov and co-workers.[36,58–61] This function again starts with a set of RKR (or *ab initio*, or other) potential points and uses a cubic spline through those points to define a unique smooth function over their range. The least-squares fitting procedure then optimizes the energies of those turning points, which are in effect the "parameters" defining the potential. We call this type of function a "spline-pointwise potential" (SPP). A key strength of this form is its model-free nature—it can treat any shape of potential energy curve without the intrinsic limitations imposed by choice of a particular analytic form, and it has been successfully applied to analyses of data for a number of standard (normal single-well potential) and nonstandard (double-minimum, shelf-state, or barrier potential) cases.[27,36,58–62] On the other hand, it suffers from some of the drawbacks associated with the original PCPP approach, in that the potential is defined by a lengthy list of many-digit turning points, and extrapolation beyond the experimental data region is problematic. This SPP form has been used in a recent analysis of the $B\,^1\Pi_u$ state of $^{7,7}Li_2$,[27] and the comparison with those

results presented in Sec. IV D delineates some of the relative strengths and weaknesses of that approach.

The third type of potential function form used for fitting spectroscopic data is what we call a "fully analytic potential" (FAP), which is based on a closed-form analytic expression defined by a modest number of parameters. The oldest flexible function of this type is probably Dunham's classic power series expansion[63]

$$V_{\rm Dun}(r) = a_0\xi^2(1 + a_1\xi + a_2\xi^2 + a_3\xi^3 + \cdots), \tag{23}$$

where $\xi = \xi_{\rm Dun} = (r - r_e)/r_e$. Because of its unphysical behavior at large distances, alternate versions of the expansion variable in this expression were proposed by Simons *et al.*[64] $\xi_{\rm SPF} = (r - r_e)/r$, by Thakkar[65] $\xi_{\rm T}(\mathrm{p};r) = \mathrm{sgn(p)}[1 - (r_e/r)^{\rm p}]$, and by Ogilvie[66] $\xi_{\rm OT} = 2(r - r_e)/(r + r_e)$. However, although the nature of those variables means that the resulting polynomial potentials will approach some finite limiting value as $r \to \infty$, the extrapolation properties of the resulting functions are often quite unrealistic. It is possible to constrain such functions to agree with a specified known dissociation energy $\mathfrak{D}_{\rm e}$ and even to have a chosen inverse-power asymptotic long-range behavior and asymptotic potential coefficient. However, imposition of the requisite constraints requires the addition of several high-order polynomial coefficients which can all too readily give rise to spurious extrema on the interval between the data region and the long-range limit.[66]

The above problems are partly resolved by use of the generalized expansion variable introduced by Šurkus *et al.*,[67] $\xi_{\rm S}(\mathrm{p};r) = \mathrm{sgn(p)}(r^{\rm p} - r_e^{\rm p})/(r^{\rm p} + a_s r_e^{\rm p})$, where $\mathrm{sgn(p)} = +1$ or -1, respectively, for p being positive or negative. For appropriate choices of the control parameters p and a_s it yields each of the variables mentioned above, and if p is fixed at the power of the known asymptotically dominant inverse-power contribution to the potential, this form automatically gives the correct long-range functional behavior, without introducing any additional constraints. Imposing externally determined values of the associated long-range potential coefficient and/or dissociation energy $\mathfrak{D}_{\rm e}$ does introduce additional constraints on the coefficients of the analog of Eq. (23). However, the fact that the long-range behavior typically requires $3 \leqslant \mathrm{p} \leqslant 6$ means that the variable $\xi_{\rm S}$ tends to approach its limiting values (of ± 1) at relatively small values of $|(r - r_e)/r_e|$, so use of such constraints is relatively unlikely to introduce spurious behavior between the data region and the asymptote.[23] On the other hand, for the larger values of $\mathrm{p} = 5$ or 6 usually required by the nature of the long-range potential for neutral molecules, this same property will substantially reduce the flexibility of the potential function at large values of r/r_e, which will limit its ability to describe data for levels spanning a large fraction of the potential well.

In the past decade, a number of flexible FAP functions have been developed and applied in direct-potential-fit data analyses and have proved capable of accurately representing very-high-resolution data spanning very large fractions of the potential well. Some of the most effective and flexible of these model potentials are generalizations of the familiar Morse potential (with acronyms GMO, MMO, and EMO),[6,8,11,15] or a combined Morse–Lennard-Jones (MLJ) form,[21] in all of which a Morse potential type of exponent coefficient is expanded as a power series in some radial variable. In this case, the least-squares procedure optimizes the parameters characterizing the chosen analytic function. However, while these forms can describe both standard single-minimum potentials and nonstandard double-minimum or shelf-state functions,[21,22] none of them can describe a potential with a barrier which protrudes above the potential asymptote. Moreover, these forms cannot incorporate more than one inverse-power long-range term, and all of the forms introduced to date sometimes encounter problems in extrapolating across the interval between the experimental data region and the potential asymptote. Simple but powerful means of addressing these problems are presented below.

One means of representing a potential with a barrier was introduced by Tellinghuisen and successfully applied to the $B\,0^+$ ($^3\Pi$) State of BrCl.[68] It treats the barrier as the result of an avoided crossing between a repulsive and an attractive potential. However, that approach requires one to introduce parameters to characterize both the two potentials and an r-dependent interstate coupling function, and unless one has data directly dependent on the upper adiabat curve as well as on the potential with a barrier, the resulting description will have a tendency to be overparametrized and nonunique.

B. "Double-exponential-long-range" potential form

The model potential introduced here resolves all of the problems outlined above. This "double-exponential-long-range" (DELR) potential energy function consists of a Morse-type pair of exponential terms plus a user-selected analytical function to represent long-range behavior:

$$V_{\rm DELR}(r) = [\mathrm{A}e^{-2\beta(y_{\rm p})\cdot(r - r_e)} - \mathrm{B}e^{-\beta(y_{\rm p})\cdot(r - r_e)} + \mathfrak{D}_{\rm e}] + V_{\rm LR}(r), \tag{24}$$

where $V_{\rm LR}(r)$, which may be attractive or repulsive, is the function chosen to represent the long-range region. The exponent coefficient $\beta(y_{\rm p})$ is represented by a simple polynomial

$$\beta(y_{\rm p}) = \beta_0 + \beta_1 y_{\rm p} + \beta_2 y_{\rm p}^2 + \beta_3 y_{\rm p}^3 + \cdots, \tag{25}$$

and the expansion variable $y_{\rm p} = y_{\rm p}(r) = (r^{\rm p} - r_e^{\rm p})/(r^{\rm p} + r_e^{\rm p})$ is a special case of the Šurkus variable[67] in which p is a small positive integer and $a_s = 1$. The DELR preexponential coefficients A and B are defined in terms of the position r_e and depth $\mathfrak{D}_{\rm e}$ (relative to the potential asymptote) of the potential minimum by the requirements that $V_{\rm DELR}(r_e) = 0$ and $dV_{\rm DELR}(r)/dr|_{r=r_e} = 0$, which implies that

$$\mathrm{A} = \mathfrak{D}_{\rm e} + V_{\rm LR}(r_e) + V'_{\rm LR}(r_e)/\beta_0, \tag{26}$$

$$\mathrm{B} = 2\mathfrak{D}_{\rm e} + 2V_{\rm LR}(r_e) + V'_{\rm LR}(r_e)/\beta_0, \tag{27}$$

where $V'_{\rm LR}(r_e) \equiv dV_{\rm LR}/dr|_{r=r_e}$.

Note that if $V_{\rm LR}(r) \equiv 0$, $\mathrm{A} = \mathfrak{D}_{\rm e} = \mathrm{B}/2$ and this function becomes the simple "extended Morse oscillator" (EMO) function of Refs. 11 and 19. However, other choices of $V_{\rm LR}(r)$ will allow it to represent the outer repulsive wall of a potential with a barrier, a several-term attractive inverse-power long-range potential, or even the outer well of a

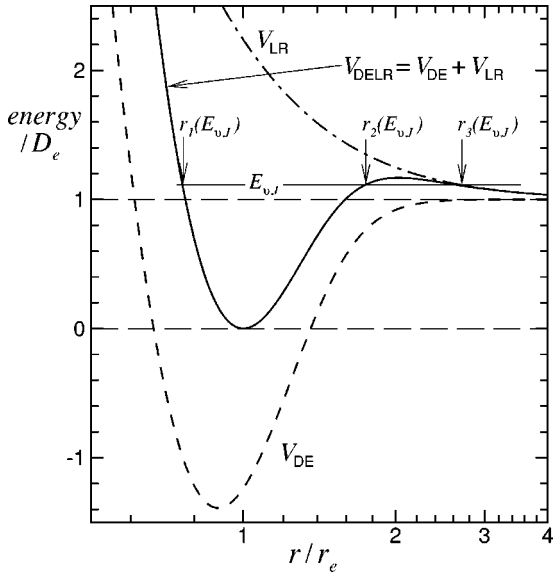

FIG. 1. Schematic illustration of the form of a DELR potential function for representing a barrier-state potential (solid curve) and its components (dashed and dot-dashed curves) and definition of the turning points associated with tunneling-predissociation level $E_{v,J}$.

double-minimum or shelf-state potential. For the first of these cases, Fig. 1 schematically illustrates the contributing components (dashed and dash-dotted curves) and the resulting overall $V_{\rm DELR}(r)$ potential function (solid curve). Note too that the exponential long-range behavior of the ''double-exponential'' (DE) contribution to Eq. (24) means that $V_{\rm DE}(r)$ will die off exponentially rapidly at long range, so that the $V_{\rm LR}(r)$ term will become dominant there.

One of the key results of Ref. 23 was the discovery that use of the expansion variable $y_{\rm p}(r)$ with $p \gtrsim 3$ suppresses most spurious extrapolation behavior for potential functions based on exponential terms with distance-dependent exponent parameters, such as Eq. (24) or the various extended Morse or Morse–Lennard-Jones functions mentioned earlier. This also proved true here with regard to extrapolation to large r. However, even with the use of this variable, the fairly high-order exponent polynomials required when the data are sensitive to the potential over a broad interval can give rise to extrapolation problems at small distances. This is not surprising, since the characteristic asymmetry of potential wells means that most of the expansion coefficients in Eq. (25) are required for defining the shape of the $\beta(y_{\rm p})$ function for $r > r_e$, while for $r < r_e$ spectroscopic data are usually only sensitive to the potential on the relatively narrow interval $r/r_e \gtrsim 0.8$, and the high-order expansion coefficients whose contribution are negligible there could cause substantial mischief on extrapolation to smaller distances.

A simple means of addressing this problem, when it arises, is to truncate the polynomial representing $\beta(y_{\rm p})$ at lower order for $r < r_e$ than for $r \geqslant r_e$:

$$\beta(y_{\rm p}) = \sum_{i=0}^{N_S} \beta_i y_{\rm p}^i \quad \text{for } r < r_e, \tag{28}$$

$$\beta(y_{\rm p}) = \sum_{i=0}^{N_L} \beta_i y_{\rm p}^i \quad \text{for } r \geqslant r_e, \tag{29}$$

where $N_S \leqslant N_L$ and the coefficients β_0 to β_{N_S} are identical in the two expansions. For $N_S \neq N_L$ this means that the (N_S+1)th derivative with respect to r, both of $\beta(y_{\rm p})$ and [when $V_{\rm LR}(r) \neq 0$] of the potential itself, will both be discontinuous at $r = r_e$. However, N_S will generally be fairly large ($N_S \gtrsim 5$), so this is not a very serious deficiency. We will see in Sec. IV how this modification of Eq. (25) can remove spurious extrapolation behavior at small distances. Note too that for the generalized Morse and MLJ potential forms discussed above, their algebraic structure means that for $N_S \neq N_L$, discontinuities at $r = r_e$ will only occur for derivatives of the potential of order (N_S+2) or higher.

A particularly useful form for $V_{\rm LR}(r)$ is the general inverse-power expansion for a long-range potential,

$$V_{\rm LR}(r) = \mathfrak{D} + \sum_{m \geqslant n} {\rm D}_m(r) C_m / r^m, \tag{30}$$

where $\mathfrak{D}$ is the energy at the potential asymptote. The nature of the atomic species yielded on dissociation determines which (positive integer) powers of m contribute to this sum and sometimes also their algebraic sign,[69–71] while accurate theoretical values of the long-range C_m coefficients have been reported for many molecular states. It is well known that the simple inverse-power asymptotic behavior of long-range dispersion energies are damped at smaller distances where the electronic wave functions of the interacting species begin to overlap significantly.[72–74] Following Douketis *et al.*,[75,76] the damping functions ${\rm D}_m(r)$ are introduced to take account of the shrinking strengths of these inverse-power terms as r decreases and to prevent them from becoming singular at $r = 0$. The present work uses the ''universal'' damping functions of Ref. 76,

$${\rm D}_m(r) = [1 - \exp\{-3.97(\rho_{\rm d} r)/m - 0.39(\rho_{\rm d} r)^2/\sqrt{m}\}]^m, \tag{31}$$

where r has units Å and $\rho_{\rm d}$ is a system-dependent scaling factor defined in terms of the ratios of the ionization potentials of the atoms forming the molecule of interest to that of the hydrogen atom;[76,77] for B-state Li_2, which dissociates to Li(2s)+Li(2p), $\rho_{\rm d} = 0.4647$. Of course other damping function expressions[78,79] or entirely different types of expressions for $V_{\rm LR}(r)$ could be used equally well in the DELR potential form.

In concluding this discussion, we note that the ${\rm D}_m(r)$ functions of Ref. (76) were derived for dispersion interactions involving $m = 6$, 8, and 10 terms, and there have been (to our knowledge) no studies of the damping behavior of first-order C_3/r^3 interaction energies. In the present case, however, $0.99 \leqslant {\rm D}_3(r) \leqslant 1.0$ for $r > 6$ Å, and at smaller distances any defects in our representation of this leading long-range term may be compensated for by the exponential-term contributions to Eq. (24).

C. BOB and Λ-doubling radial strength function

Optimal representations of the (''adiabatic'') potential energy and (nonadiabatic) centrifugal BOB function of

Eqs. (1)–(3) which incorporate physically appropriate limiting constraints were presented and tested in Ref. 20. Both functions have the same form and are defined in terms of the Šurkus-type radial expansion variable introduced above:[33]

$$\tilde{S}^A_{\rm ad}(r)=[1-y_m(r)]\sum_{i=0} u_i^A[y_{\rm p}(r)]^i+u_\infty^A y_m(r), \tag{32}$$

$$\tilde{R}^A_{\rm na}(r)=[1-y_{\rm p}(r)]\sum_{i=0} t_i^A[y_{\rm p}(r)]^i, \tag{33}$$

where m and p are selected positive integers, and the equilibrium distance r_e appearing in the definitions of $y_{\rm p}(r)$ and $y_m(r)$ is the value for the reference isotopomer, $\alpha=1$. As discussed in Ref. 20, the value of the integer power p (typically p=2–4) is chosen to yield power series expansions which will "behave well" (i.e., will rapidly achieve their limiting values without implausible excursions) in the extrapolation regions beyond the range of distances spanned by the data used in the analysis. The other integer power "m" appearing in Eq. (32) allows the asymptotic inverse-power behavior of the potential to also be imposed on this BOB potential correction function. In particular, when the potential energy function has the theoretically-predicted inverse-power long-range behavior of Eq. (30), the power defining the variable $y_m(r)$ in Eq. (32) should be set at $m=n$, the power of the leading term in that expansion. Alternately, if the potential itself does not asymptotically have inverse-power behavior, for the sake of simplicity one should simply fix $m=$p.

As is evident from the form of Eq. (32), $\lim_{r\to\infty}\tilde{S}^A_{\rm ad}(r)=u_\infty^A$ and $\tilde{S}^A_{\rm ad}(r_e)=u_0^A$. If the given molecular state dissociates to yield a ground-state atom of species A, the coefficient $u_\infty^A=0$, while if that state dissociates to yield atom A in excited state s^*, for a heteronuclear molecule,

$$u_\infty^A=\lim_{r\to\infty}\tilde{S}^A_{\rm ad}(r)=(M_A^{(\alpha)}/\Delta M_A^{(\alpha)})\,\delta E_A^{(\alpha)}(s^*), \tag{34}$$

where $\delta E_A^{(\alpha)}(s^*)$ is the atomic isotope shift (relative to isotopomer $\alpha=1$) of the energy associated with a transition from the ground state to excited state s^* for atom A of isotopomer-α.[20] For the present case of a homonuclear diatomic dissociating to one excited-state and one ground-state atom, this limiting constraint is

$$u_\infty^A=\frac{M_A^{(\alpha)}}{2\Delta M_A^{(\alpha)}}\,\delta E_A^{(\alpha)}(s^*). \tag{35}$$

Similarly, u_0^A determines the contribution of atom A to the energy shift of the potential minimum from the reference isotopomer to isotopomer-α. In general u_∞^A is known and is either zero (for ground-state atoms) or quite small, while u_0^A is determined empirically from the isotopomer dependence of the well depth or (for excited electronic states) of the electronic energy T_e of that state.[20]

The recommended functional form for the centrifugal BOB correction function, Eq. (33), incorporates the physically necessary constraint that $\lim_{r\to\infty}\tilde{R}^A_{\rm na}(r)=0$,[20] while $\tilde{R}^A_{\rm na}(r_e)=t_0^A$. As discussed in Ref. 20, the value of t_0^A is sometimes determined by external constraints, but when that is not the case, ambiguities inherent in the definition of the (approximate[18,29,30]) Hamiltonian of Eqs. (1) and (9) suggest that it should be fixed as $t_0^A=0$.

For the Λ-doubling radial strength function $f_\Lambda(r)$, the fact that all interatomic interactions go to zero as $r\to\infty$ means that necessarily $\lim_{r\to\infty} f_\Lambda(r)/r^4=0$. Because of the r^4 term in the denominator, this condition is clearly satisfied as long as $f_\Lambda(r)$ remains finite when $r\to\infty$. As a result, the expression used for this function is simply a power series in $y_{\rm p}(r)$:

$$f_\Lambda(r)=\sum_{i=0} l_i y_{\rm p}(r), \tag{36}$$

where the expansion coefficients $\{l_i\}$ have units $1/{\rm cm}^{-1}$. In this case we have no particular expectations regarding the value of this function at r_e, so the leading coefficient l_0 is freely determined by the fit to the experimental data. Note too that in contrast to the BOB correction functions, all of the isotopomer-mass dependence of the Λ-doubling term in Eq. (9) is contained in the centrifugal-type factor $(\hbar^2/2\mu_\alpha r^2)^2$ in Eq. (7). As a result, the coupling-strength function $f_\Lambda(r)$ is an isotopomer-independent property of the molecular state and has no individual atomic components, so there are no atom-specific labels associated with this function or its expansion coefficients.

In conclusion, we note that while it may be convenient to use the same integer power p to define the expansion variables $y_{\rm p}(r)$ in Eqs. (25) [or Eqs. (28) and (29)] and in Eqs. (32), (33), and (36), this is not essential. For example, while the data defining the overall potential may span a relatively wide range of r, the (usually) more limited amount of data available for minority isotopomers may only allow the determination of $\tilde{S}^A_{\rm ad}(r)$ for one or both of the component atoms over a narrower interval. In this case, avoidance of spurious extrapolation behavior might dictate the use of a larger value of p for the BOB correction function than for the potential itself. In the present study, however, the same value of p was used to define all of these functions.

IV. $B\,^1\Pi_U$ STATE OF Li_2

A. Overview of previous work

Of all homonuclear diatomic molecules, Li_2 is the simplest stable species that possesses an electron core, and it has been of interest theoretically[40,80–84] and experimentally[24,26,85–89] for decades. The $B\,^1\Pi_u$ state of Li_2 is well known for having a potential energy barrier due to a competition between the repulsive long-range dipole–dipole interaction and the attractive dispersion and electron exchange interaction. Modern spectroscopic studies of the $B\,^1\Pi_u$ state began with the work of Hessel and Vidal,[26] who observed the $B\,^1\Pi_u - X\,^1\Sigma_g^+$ absorption and laser-induced fluorescence spectrum of $^{7,7}Li_2$ at high resolution. They determined molecular constants using a Dunham analysis and a potential function from a quantum-mechanical DPF analysis using a pointwise "PCPP" potential form. Their analysis yielded an estimated B-state well depth (from the minimum to the as-

ymptote, a value based on $\mathfrak{D}_e$ for the X state) of $\mathfrak{D}_e(B) = 3068(\pm 150)$ cm^{-1} and a potential barrier height of 450 (± 50) cm^{-1}.

Some years later Russier *et al.*[24] reported high-resolution Fourier transform spectra of the $F\,^1\Sigma_g^+ \rightarrow B\,^1\Pi_u$ fluorescence of $^{7,7}Li_2$ and $^{6,6}Li_2$, including transitions into a range of rotational sublevels for the highest ($v=17$ for $^{7,7}Li_2$) or second-highest ($v=15$ for $^{6,6}Li_2$) vibrational levels below the barrier maximum. Extrapolation of near-dissociation expansion expressions for the level energies yielded barrier heights of 498(± 1) and 499(± 2) cm^{-1} for the two isotopomers, and the combination of an RKR potential for the well with a theoretical inverse-power long-range tail gave very similar values. While they were not included in the analysis, calculated tunneling predissociation level widths obtained from those potentials were in reasonable agreement with the experimental values which had been obtained for levels with widths $\gtrsim 0.1$ cm^{-1}.

More recently, Bouloufa *et al.*[25] measured several hundred $B\,^1\Pi_u \leftarrow X\,^1\Sigma_g^+$ transitions for $^{7,7}Li_2$ and $^{6,6}Li_2$ at higher resolution, including many transitions into quasibound or tunneling-predissociation levels whose widths (or decay lifetimes) were also measured. Bouloufa *et al.*[27] later also reported an analysis in which level energy data for the f-parity $B\,^1\Pi_u$ levels of the $^{7,7}Li_2$ isotopomer were combined with data from Hessel and Vidal[26] and Russier *et al.*[24] to determine a full potential energy function for this isotopomer from a direct-potential-fit approach using the SPP pointwise potential form of Pashov and co-workers.[36,58–61] The resulting potential has a barrier height in good agreement with those of Russier *et al.*,[24] and it gave reasonable predictions of the observed tunneling predissociation linewidths.[27] However, that analysis took no account of BOB effects, considered only data involving the unperturbed f-parity Λ-doubled levels, and while the level width data were tested against the new potential, they were not used in its determination. Moreover, the SPP functional form they used for the potential has some drawbacks (see below).

B. Experimental data used in the present analysis

The present analysis is based on several kinds of data. For $^{7,7}Li_2$ the data came from the same three sources as in Ref. 27: (i) synthetic $B-X$ transitions generated from the constants of Hessel and Vidal,[26] spanning the range $v'(B) = 0-4$ and $J'(B) = 1-50$, (ii) the more accurate $B-X$ transition energies obtained by Bouloufa *et al.*,[25] and (iii) lower-resolution $F-B$ fluorescence data of Russier *et al.*[24] As in Ref. 27, to simplify the analysis and reduce possible systematic calibration errors, combination differences were used to convert the $^{7,7}Li_2$ $F-B$ fluorescence data to artificial $B-X$ transition energies.[90] However, while the analysis of Ref. 27 considered only data involving the unperturbed f-parity levels, the present analysis utilizes all available data for both e- and f-parity levels. All observed predissociation-broadened lines, weighted by appropriate uncertainties (see below), were included in the present analysis.

Since our object here is to determine the properties of the $B\,^1\Pi_u$ state, we followed the approach of Ref. 27 and decoupled our analysis from a determination of ground-state properties by using their refined $X\,^1\Sigma_g^+$ constants to define all $B-X$ transition frequencies as originating at their (extrapolated) ground-state potential minimum for $^{7,7}Li_2$. In other words, the energies of the lower levels of the $B-X$ transitions were calculated from the X-state Dunham constants in Table I of Ref. 27 (including their $Y_{0,0}$ value) and $B-X$ transitions treated as if they originated at the potential minimum of the $X\,^1\Sigma_g^+$ state of isotopomer $^{7,7}Li_2$. The natural zero of energy in any combined isotopomer analysis is the dissociation limit yielding ground-state atoms,[20] and on this scale the ground-state potential minimum lies at an energy of $-\mathfrak{D}_e(X) = -8516.78(\pm 0.10)$ cm^{-1}.[27,91] Combining this quantity with the $(^2S+{}^2P)$ energy asymptote for the $B\,^1\Pi_u$ state of $^{7,7}Li_2$, 14 903.983 468 cm^{-1},[92] and the value of $T_{0e}(B\,^1\Pi_u) = 20\,570.8877$ cm^{-1} determined in Ref. 27 yields the dissociation energy $\mathfrak{D}_0(B\,^1\Pi_u) = 2849.8758$ cm^{-1}. Finally, combining this value with the calculated vibrational zero-point energy on our fitted model potential (134.568 cm^{-1}) yields $\mathfrak{D}_e(B) = 2984.444$ (± 0.11) cm^{-1}. As in Ref. 27, this quantity was held fixed in the present single-state analysis.

The $F\,^1\Sigma_g^+ \rightarrow B\,^1\Pi_u$ transition frequency data for the less abundant isotopomers were also included in a manner which decouples study of the $B\,^1\Pi_u$ state from the properties of the $F\,^1\Sigma_g^+$ state, since the latter is known to be perturbed. In particular, all transitions originating in a given F-state level were treated as an independent fluorescence series, with the term values for those F-state levels being parameters determined by the analysis. This additional minor-isotopomer data consisting of 1039 transitions from 60 such series for $^{6,6}Li_2$ and 277 data from 11 series for $^{6,7}Li_2$ (mostly unpublished) was generously provided by Martin and Ross.[28] These high-quality data are a critical component of the present analysis, since it is their inclusion which allows a determination of the BOB potential energy correction function.

In addition to the above, the data set utilized in the present analysis included 30 tunneling predissociation widths for $^{7,7}Li_2$ reported by Bouloufa *et al.*[25] and 19 additional widths for broader levels from Ref. 24, together with 20 widths for $^{6,6}Li_2$ obtained from the results of Russier *et al.*[24,93] (The narrower $^{7,7}Li_2$ linewidths reported in Ref. 24 were superceded by the more accurate values of Ref. 25.) This data set omits three of the widths reported in Ref. 25, as they give anomalously large discrepancies in any of the calculations performed here or reported in Ref. 25 or 27 and are believed to be unreliable. The widths used in our fits were all weighted by relative uncertainties of 14%, a value based on an assumed experimental uncertainty of 10% and computational uncertainty (see Sec. II B) of 10%. Similarly, uncertainties associated with transition frequencies involving predissociating levels were taken as the larger of the normal uncertainty for that set of experiments (e.g., 0.002 cm^{-1} for the data of Ref. 25) or 14% of the associated line width. This estimate allows for an uncertainty contribution of $0.10\times\Gamma$ from the computational method used for locating the quasibound level and an additional $0.10\times\Gamma$ associated with determining the centers of the broadened lines. The data set used

TABLE I. Summary of the experimental data for $B\,^1\Pi_u$ state Li_2 used in the present analysis.

Isotopomer	Electronic transition	Transition energies: No. lines e	No. lines f	v range	J range	unc./ cm^{-1}	Linewidths[a]: No. widths e	No. widths f	v range	Source Ref.
$^{7,7}Li_2$	$B\,^1\Pi_u \rightarrow X\,^1\Sigma_g^+$	694	350	0–4	1–50	0.005	-	-	-	26
	$B\,^1\Pi_u \leftarrow X\,^1\Sigma_g^+$	348	176	3–16	1–72	0.002	30	-	10–16	25
	$F\,^1\Sigma_g^+ \rightarrow B\,^1\Pi_u$	125	144	5–17	1–36	0.01	19	-	15–17	24
$^{6,7}Li_2$	$F\,^1\Sigma_g^+ \rightarrow B\,^1\Pi_u$	181	96	0–16	12–31	0.005	-	-	-	28
$^{6,6}Li_2$	$F\,^1\Sigma_g^+ \rightarrow B\,^1\Pi_u$	676	363	0–15	1–41	0.005	12	8	13–15	24, 28

[a]Relative uncertainties of ±14% were assumed for all widths.

in this analysis is summarized in Table I and may be obtained from this journal's electronic data archive.[94]

Finally, we note that some very recent work on the mixed isotopomer $^{6,7}Li_2$ reported accurate new $B-X$ transition energies and B-state predissociation widths for a wide range of levels.[95,96] In that case, however, the overwhelmingly dominant predissociation mechanism was gerade–ungerade symmetry breaking which allows Feschbach-type predissociation into the continuum above the asymptote of the $1\,^1\Pi_g$ state. Since this does not depend on the B-state potential alone, these widths could not be used in the present analysis. Similarly, the lack of a comprehensive combined isotopomer analysis which clearly delineates BOB effects in the $X\,^1\Sigma_g^+$ state prevented our use of their transition energy data in the present work.

C. DPF analysis of the $B\,^1\Pi_u$ state of Li_2

The present section describes the results obtained using non-linear least-squares fits to the experimental data of Table I to determine parameters characterizing the DELR potential of Eqs. (24)–(31), the BOB correction functions of Eqs. (32) and (33), and the Λ-doubling radial strength function of Eq. (36), for the $B\,^1\Pi_u$ state of Li_2. In these fits $^{7,7}Li_2$ was chosen as the reference isotopomer ($\alpha=1$), and since most of the nearby Σ states have $^1\Sigma_u^+$ symmetry, we define the factor $sg(e,f)$ in Eq. (9) to be zero for f-parity levels and $+1$ for e-parity rotational sublevels. In other words, we assume that the former are unperturbed and only the latter are affected by electronic–rotational angular momentum interactions.

The theory of long-range interactions shows that for this state the leading contributions to Eq. (30) correspond to $m=3$, 6, 8, and 10, and since reliable values of the associated potential coefficients have been reported, these four terms were used to define the $V_{LR}(r)$ component of our DELR model for the potential energy function. It is, of course, the positive (repulsive) value of C_3 which gives rise to the barrier in this state. The present analysis utilizes the values of these coefficients quoted in Ref. 27, converted to units cm^{-1} Å^m and rounded (see Table III), and as indicated earlier, the dimensionless scaling parameter used to define the damping functions of Eq. (31) is $\rho_d=0.4647$. Since the asymptotically dominant term in the long-range potential for this state has (inverse) power $n=3$, the integer m in Eq. (32) was set at $m=n=3$. In addition, the accurately known $Li(2p)\leftarrow Li(2s)$ atomic isotope shift[92] shows that relative to ground-state atoms, the B-state asymptote for $^{6,6}Li_2$ lies $0.351\,352\,(\pm 0.000\,015)$ cm^{-1} below that for $^{7,7}Li_2$. Equation (35) then yields $u_\infty^{Li}=1.055\,78(5)$ as the limiting asymptotic value of the BOB potential correction function $\Delta V_{ad}^{Li}(r)$ for states associated with this limit.

The final parameter which must be selected to specify the form of our potential energy and related functions is the power p used to define the expansion variable $y_p(r)$. The work of Refs. 20 and 23 showed that p values of 2–4 often give the best extrapolation properties, and since the integer power m in Eq. (32) must be fixed at $m=n=3$, for the sake of simplicity we also fixed $p=3$ in the definition of the expansion variables used to define the potential energy function, the BOB correction functions and the Λ-doubling radial strength functions used herein.

In the initial fits, the simple power series of Eq. (25) was used to define the $\beta(y_3)$ exponent parameter of the DELR potential [i.e., $N_L=N_S$ in Eqs. (28) and (29)]. After some experimentation it was determined that a "good" fit (i.e., a fit yielding rmsr$\lesssim$1 and requiring a minimum number of free parameters) was obtained using a polynomial of order 9 for the exponent coefficient $\beta(y_p)$, and polynomial orders of 1 for the adiabatic potential energy BOB functions of Eqs. (32) and 2 for the Λ-doubling functions of Eqs. (36). With the value of the centrifugal BOB correction function constrained to be zero at r_e, $t_0^{Li}=0$, freeing higher-order parameters (t_1^{Li}, t_2^{Li},…, etc.) had very little effect on the quality of fit, which indicates that the nonadiabatic centrifugal BOB correction function is too weak to be determined from the existing data for this system. Such terms are therefore omitted in the rest of the present analysis.

Although the above parameter set yielded potential energy and correction functions which gave a good fit to the experimental data (rmsr=0.948), the {9,9} plot in the lower segment of Fig. 2 shows that the short-range extrapolation behavior of the $N_L=N_S=9$ DELR potential function obtained in this way is unsatisfactory. This led us to apply Eqs. (28) and (29) and use different orders for the polynomial representing $\beta(y_p)$ when $r<r_e$ versus when $r>r_e$. Repeating the fits using N_S values ranging from 1 to 8 yielded the results summarized in Table II and illustrated in Fig. 2. The lower segment of Fig. 2 shows that unphysical short-range extrapolation behavior occurs for $N_S\geqslant 6$, and the upper segment shows that this is due to a too-steep falloff of the associated $\beta(y_3(r))$ function at small distances, outside the data-sensitive region. On the other hand, for $N_S\leqslant 5$ the short-range repulsive wall of the potential energy function is

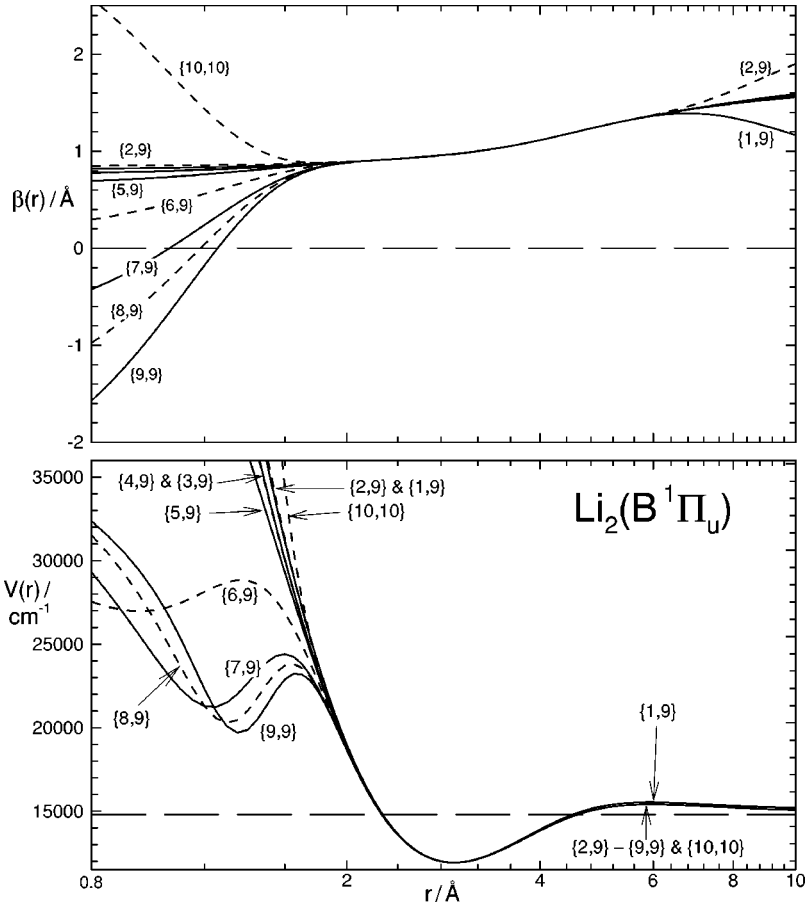

FIG. 2. Lower: Fitted DELR potential energy functions obtained for various choices of the exponent polynomial orders $\{N_S, N_L\}$. Upper: plots of the $\beta(y_3(r))$ exponent coefficient functions defining these potential energy functions. Both: curves corresponding to odd and even values of N_S, are drawn as solid or dashed curves, for the sake of clarity.

always well behaved. This demonstrates that allowing for separate power-series orders in Eqs. (28) and (29) is indeed a successful means of suppressing unphysical potential function extrapolation behavior at small distances. Note that while the maximum powers used in the exponent polynomials differ for $r>r_e$ and $r<r_e$, there is a single common set of expansion coefficients $\{\beta_i\}$, so the total number of free parameters in the fits does not depend on N_S.

The N_S dependence of the rmsr values in Table II can be readily explained in the following way. For the very small values $N_S=1$ or 2, the exponent polynomial defining the shape of the potential energy function for $r<r_e$ has very little flexibility, so the quality of fit is expected to be quite poor, as seen in Table II. For intermediate N_S values of 3–5, the low-order terms provide $\beta(y_p)$ with good flexibility at modest $|r-r_e|$ while the higher-power terms are free to accurately characterize $\beta(y_p)$ at larger values of $r>r_e$. However, some of those higher-power terms tend to yield inappropriate behavior at small r, and when setting $N_S>5$ allows such terms to contribute to $\beta(y_p)$ at $r<r_e$, some of the flexibility in the large-r region is sacrificed to the essential requirement that the function remain well behaved on the data-sensitive portion of the $r<r_e$ region. This is the reason for the increase in RMSR when $N_S\geqslant 6$. This explanation is supported by the fact that giving the $\beta(y_p)$ function more overall flexibility by using an $\{N_S, N_L\}=\{10,10\}$ expansion yielded both a potential which is well behaved in the short-range extrapolation region (see Fig. 2) and a fit with rmsr $=0.858$, a (very) slightly smaller value than that obtained with the recommended {5,9} exponent expansion. The results in Fig. 2 also confirm that use of the power $p=3$ to define the expansion variable $y_p(r)$ successfully ensures that the $\beta(y_p(r))$ function will rapidly approach a positive asymptotic limiting value outside the data region, thus preventing spurious nonphysical potential function extrapolation behavior at large r.[23]

The results in Table II and Fig. 2 show that our optimum representation of the experimental data for the $B\,^1\Pi_u$ state of Li_2 is obtained using a DELR potential with a $p=3$ radial expansion variable $y_3(r)$ and exponent coefficient orders $N_S=5$ and $N_L=9$. Of the N_S values which yielded the best quality of fit and for which the inner-wall potential extrapolation is "well behaved" ($N_S=3-5$), this is the one which yields the highest-order analytic continuity at $r=r_e$. In par-

TABLE II. Quality of fit to all data using various choices for the exponent function power N_S of Eq. (28), with $N_L=9$.

$\{N_L, N_S\}=$	{9, 9}	{8, 9}	{7, 9}	{6, 9}	{5, 9}	{4, 9}	{3, 9}	{2, 9}	{1, 9}
rmsr(total) =	0.948	0.939	0.976	0.950	0.862	0.874	0.876	3.872	6.075

TABLE III. Recommended potential energy, BOB correction, and Λ-doubling function parameters for B-state Li_2 obtained using the DELR model potential of Eqs. (24)–(31) with an $\{N_S, N_L\}=\{5,9\}$ $\beta(y_3)$ exponent function. The fixed coefficients defining the $V_{LR}(R)$ component of the potential are (Ref. 24) $C_3=1.788\times10^5$ cm^{-1} Å^3, $C_6=-6.975\,86\times10^6$ cm^{-1} Å^6, $C_8=-1.378\times10^8$ cm^{-1} Å^8, and $C_{10}=-3.445\times10^9$ cm^{-1} Å^{10}, while $\rho_d=0.4647$. The numbers in parentheses are the 95% confidence limit uncertainties in the last significant digit shown for certain physically significant parameters.

$\mathfrak{D}_e$ (cm^{-1})	2984.444[a]		
r_e (Å)	2.936 171 42(310)		
A (cm^{-1})	3853.980 130[b]		
B (cm^{-1})	9982.620 189[b]		
β_0 (Å^{-1})	0.970 911 966	u_0^{Li} (cm^{-1})	0.747 8(550)
β_1 (Å^{-1})	0.207 535 8	u_1^{Li} (cm^{-1})	−0.472(210)
β_2 (Å^{-1})	0.175 154 2	u_∞^{Li} (cm^{-1})	1.055 78
β_3 (Å^{-1})	0.188 843		
β_4 (Å^{-1})	0.156 48	l_0	0.000 313 65(100)
β_5 (Å^{-1})	0.252	l_1	−0.000 215(15)
β_6 (Å^{-1})	−2.185	l_2	0.000 314(16)
β_7 (Å^{-1})	6.915 98		
β_8 (Å^{-1})	−9.690 347 7		
β_9 (Å^{-1})	4.718 6		
rmsr=	0.852 for the 3153 frequency data		
	1.224 for the 69 tunneling width data		
	0.862 for the 3222 data overall		

[a]Held fixed; see text.
[b]Generated from the fit parameters using Eqs. (26) and (27).

ticular, for $N_S=3$ potential function derivatives of order $\geqslant 4$ are discontinuous at $r=r_e$, while for $N_S=5$ this only occurs for derivatives of order $\geqslant 6$. The parameters defining this recommended DELR potential and the associated BOB and Λ-doubling radial strength function are listed in Table III. The barrier maximum of this recommended potential for $^{7,7}Li_2$ is located at $r=5.95$ Å and has a height of 500.07 (± 0.02) cm^{-1}, where the uncertainty is calculated from the uncertainties in the fitted potential parameters and the correlation matrix associated with the fit [see, e.g., Eq. (7) of Ref. 57]. This result is in good agreement with the value 499.94(± 0.5) cm^{-1} obtained by Bouloufa *et al.*[27] and, within their somewhat larger uncertainties, also with the ones determined by Russier *et al.*[24]

The BOB potential correction function $\tilde{S}_{ad}^{Li}(r)$ determined here shows that relative to the energy of ground state atoms, the potential minimum for $^{6,6}Li_2$ lies 0.249 (± 0.018) cm^{-1} lower (determined from the value of u_0^{Li}) and the barrier maximum some 0.303(± 0.015) cm^{-1} lower than the corresponding values for $^{7,7}Li_2$. Since the potential asymptote for $^{6,6}Li_2$ lies 0.351 352 cm^{-1} below that for $^{7,7}Li_2$,[92] this indicates that $\mathfrak{D}_e$ for $^{6,6}Li_2$ is 0.102 (± 0.018) cm^{-1} smaller and the barrier height seen by a colliding pair of $^6Li(^2S)+^6Li(^2P)$ atoms is 0.048 (± 0.008) cm^{-1} higher than the corresponding values for $^{7,7}Li_2$. On the other hand, the small magnitude of the slope of $\tilde{S}_{ad}^{Li}(r)$ at $r_e(^{7,7}Li_2)$ means that the equilibrium bond length for $^{6,6}Li_2$ is smaller than that for $^{7,7}Li_2$ by only ca. 0.000 003 5 Å, a shift of the same magnitude as the uncertainty in $r_e(^{7,7}Li_2)$ (see Table III). It is important to remember, however, that to perform accurate calculations for $^{6,6}Li_2$ or $^{6,7}Li_2$, one cannot just substitute these different $\mathfrak{D}_e$ and r_e values into our DELR function. Rather, the minor-isotopomer potential must be generated as the sum of the DELR potential of Table III plus the correction function defined by Eqs. (2) and (32).

While the above differences may seem small, they are quite significant relative to the overall quality of the fit. In particular, on repeating our combined-isotopomer analysis while neglecting the BOB potential correction function $\tilde{S}_{ad}^{Li}(r)$, the best fit achieved yielded rmsr=1.071, a value some 23% larger than that obtained when this correction function is included. To our knowledge, this is the first quantitative determination of such isotopomer potential differences for any state of Li_2.

As a test of the importance of the Λ-doubling perturbation function to our analysis, the fit using our p=3 DELR potential with $\{N_S, N_L\}=\{9,5\}$ was repeated with $f_\Lambda(r)$ set equal to zero. The best result which could be obtained in this way had rmsr(total)=18.87, a value more than 20 times larger than that for the recommended model of Table III. As a further test of our model for Λ doubling, a fit to our recommended model was also performed while inverting the assumed sign convention for sg(e,f)—i.e., while treating the e-parity levels as being unperturbed and assuming that the perturbation affects only the f-parity levels. The resulting fit gave rmsr(total)=1.408, a value some 63% larger than that obtained when the f-parity levels were treated as being "mechanical" and the e-parity levels as perturbed. This confirms both the validity of the present perturbation-potential treatment of Λ-doubling and the physical significance of the perturbation strength function determined here. It also shows that an analysis of the present type can provide a practical empirical way of determining the symmetry of the dominant perturbing state giving rise to observed Λ-doubling level splittings.

The two upper segments of Fig. 3 show our adiabatic BOB potential energy correction function $\tilde{S}_{ad}^{Li}(r)$, and the Λ-doubling radial strength function $f_\Lambda(r)$ determined by our analysis together with the associated J-independent Λ-doubling perturbation strength function for the reference isotopomer, $\Delta V_\Lambda^{(7,7)}(r)$. To put these results in context, the bottom segment of this figure shows the recommended DELR potential energy function of Table III, and the solid segments of all curves indicate the data-sensitive region. As required by their functional forms, this $f_\Lambda(r)$ function approaches some unspecified constant value as $r\to\infty$, while $\Delta V_\Lambda^{(7,7)}(r)\to 0$ and $\tilde{S}_{ad}^{Li}(r)$ approaches the limiting value u_∞^{Li} defined by the $^2P\leftarrow{}^2S$ atomic isotope shift. These functions are all smooth and behave reasonably in their extrapolation to small distances.

Level widths have not previously been used in direct determination of potential energy functions, so it seems appropriate to examine both the degree of agreement achieved and the effect of those data on the analysis. Table IV lists the experimental tunneling predissociation linewidths for this system (Γ_{obs}) and compares them with the widths calculated from the present recommended potential (Γ_{calc}). The three $^{7,7}Li_2$ entries in italic font are the Refs. 25 data omitted from our analysis because they are believed to be unreliable.

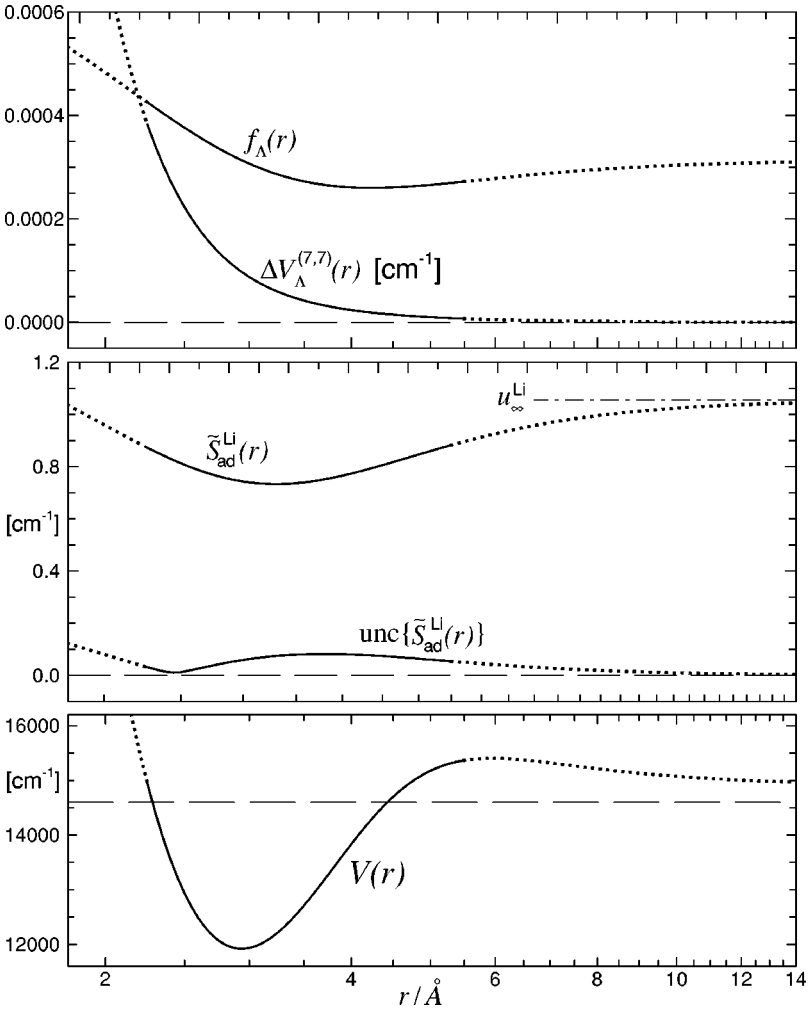

FIG. 3. Upper: Fitted dimensionless Λ-doubling radial strength function $f_\Lambda(r)$ (dimensionless), and the associated perturbation strength function $\Delta V_\Lambda^{(7,7)}(r)$ for $^{7,7}Li_2(B\,^1\Pi_u^+)$. Middle: effective adiabatic potential correction function $\tilde{S}_{\rm ad}^{\rm Li}(r)$ and its 95% confidence limit uncertainty (both in units cm^{-1}). Bottom: recommended $\{N_S,N_L\}=\{5,9\}$ DELR potential yielded by the present analysis. In all three segments, curve are solid in the data-sensitive region and dotted in the extrapolation regions.

When the fit to the same potential energy and correction function model was repeated using only the transition frequency data, the resulting potential and correction function parameters changed very little, and the quality of fit to the widths predicted by the resulting model was essentially unchanged. This result is somewhat disappointing, since it suggests that the predissociation rate data provides very little information beyond that contained in the transition frequencies. However, this result probably mainly reflects the accuracy of our theoretical model for the $V_{\rm LR}(r)$ function which determines the shape of the outer wall of the noncentrifugal potential energy barrier, and the fact that the value of $\mathcal{D}_e(B)$ is accurately known from the ground-state value, and hence was not a free parameter in our fits. These conditions will not be true in general, so the techniques for practical treatment of tunneling lifetime data presented in Sec. II B may be of considerable importance in other cases. In any case, while the predissociation level widths do not appear to provide crucial constraints on the present analysis, they do confirm the validity of our recommended potential energy and correction functions.

D. Comparison with previous work: Spline-pointwise model potential versus our fully analytic DELR potential

As mentioned earlier, the spline-pointwise potential (SPP) model introduced by Pashov and co-workers[36,58–61] has been used very successfully in a number of data analyses, both for states with a simple single minimum and for nonstandard double-minimum, shelf-state, or barrier-potential cases. One objective of the present work was to compare that approach with the present one in which the analysis is based on a fully analytic (''FAP'') potential function. The present analysis was therefore repeated using the same restricted data set used in the SPP-model analysis of Ref. 27, 712 transition energies involving f-parity levels of $^{7,7}Li_2$. For these data only the DELR potential function and the centrifugal BOB correction function needed to be considered, since $\tilde{S}_{\rm ad}^{(\alpha)}(r)$ has no relevance when dealing with data for a single isotopomer, and the effect of Λ doubling cannot be discerned when considering data for only a single e/f parity.

The potential used for these tests was the recommended $\{N_S,N_L\}=\{5,9\}$ DELR function, and as above, the effects of the centrifugal BOB function $g^{(\alpha)}(r)$ were found to be negligible. The last column of Table V shows the quality of agreement of these data with the recommended potential of Table III, and the second to last column shows the agreement obtained when its parameters were refined by a fit to the 712 transition frequencies. Comparisons with the middle column of this table shows that the quality of agreement obtained using the SPP potential of Ref. 27 is distinctly worse than that yielded by the DELR potential. The reasons for this

TABLE IV. Comparison of calculated and observed tunneling predissociation level widths for the $B\,^1\Pi_u$ state of Li_2. The uncertainty used to weight each of these data in the fits was $unc(\Gamma)=0.14\times\Gamma_{obs}$. The level energies $E_{v,J}$ are expressed relative to the isotopomer-independent asymptote of the ground $X\,^1\Sigma_g^+$ state, which dissociates to ground-state atoms.[a]

v	J	p	$E_{v,J}\,(cm^{-1})$	$\Gamma_{calc}\,(cm^{-1})$	$\Gamma_{obs}\,(cm^{-1})$	$\frac{\Gamma_{calc}-\Gamma_{obs}}{unc(\Gamma)}$
For the {7, 7} isotopomer						
10	62	*e*	15904.750	0.008 81	0.009 423	−0.46
11	54	*e*	15710.885	0.000 0615	0.000 095	−2.50
11	*56*	*e*	*15783.338*	*0.003 09*	*0.001 7*	*5.80*
12	*49*	*e*	*15652.779*	*0.000 380*	*0.000 117*	*15.9*
13	41	*e*	15526.330	0.000 0266	0.000 034	−1.55
13	*43*	*e*	*15580.997*	*0.000 871*	*0.000 5*	*5.26*
13	44	*e*	15608.588	0.004 41	0.003 15	2.84
13	45	*e*	15636.240	0.020 4	0.019 4	0.38
13	46	*e*	15663.833	0.085 5	0.100	−1.03
14	35	*e*	15485.197	0.000 331	0.000 345	−0.29
14	36	*e*	15507.709	0.001 44	0.001 27	0.95
14	37	*e*	15530.467	0.005 92	0.005 57	0.45
14	38	*e*	15553.403	0.022 8	0.023 1	−0.09
14	39	*e*	15576.423	0.081 4	0.079	0.22
15	25	*e*	15396.036	0.000 119	0.000 11	0.59
15	26	*e*	15412.235	0.000 389	0.000 414	−0.43
15	27	*e*	15428.859	0.001 25	0.001 11	0.90
15	28	*e*	15445.871	0.003 93	0.003 51	0.85
15	29	*e*	15463.229	0.012 0	0.011 5	0.33
15	30	*e*	15480.878	0.035 6	0.036 4	−0.16
15	31	*e*	15498.752	0.100	0.108	−0.50
15	32	*e*	15516.766	0.267	0.51	−3.37
15	33	*e*	15534.822	0.661	0.68	−0.20
16	10	*e*	15328.254	0.000 137	0.000 122	0.87
16	11	*e*	15335.007	0.000 234	0.000 196	1.38
16	12	*e*	15342.335	0.000 415	0.000 43	−0.25
16	13	*e*	15350.225	0.000 757	0.000 78	−0.21
16	14	*e*	15358.664	0.001 42	0.001 58	−0.71
16	15	*e*	15367.637	0.002 74	0.004 72	−2.98
16	16	*e*	15377.126	0.005 37	0.006 3	−1.05
16	17	*e*	15387.112	0.010 7	0.008 92	1.42
16	18	*e*	15397.570	0.021 6	0.023 8	−0.67
16	19	*e*	15408.473	0.043 6	0.041 3	0.40
16	20	*e*	15419.786	0.088 1	0.074 1	1.34
16	21	*e*	15431.470	0.176	0.180	−0.14
16	22	*e*	15443.477	0.347	0.33	0.36
16	23	*e*	15455.757	0.663	0.70	−0.38
16	24	*e*	15468.262	1.22	1.3	−0.42
16	25	*e*	15480.961	2.16	2.6	−1.20
16	26	*e*	15493.856	3.65	4.	−0.62
16	27	*e*	15506.834	5.84	8.	−1.92
17	1	*e*	15382.107	0.692	0.80	−0.96
17	2	*e*	15383.136	0.732	0.91	−1.39
17	3	*e*	15384.675	0.794	0.85	−0.46
17	4	*e*	15386.719	0.885	1.1	−1.39
17	5	*e*	15389.261	1.01	1.1	−0.58
17	6	*e*	15392.293	1.18	1.2	−0.13
17	7	*e*	15395.807	1.40	1.4	0.02
17	8	*e*	15399.787	1.70	1.9	−0.75
17	9	*e*	15404.223	2.09	1.9	0.71
17	11	*e*	15414.423	3.27	3.6	−0.65
17	12	*e*	15420.163	4.14	4.6	−0.72
For the {6, 6} isotopomer						
13	35	*e*	15556.603	0.066 7	0.078	−1.03
13	36	*e*	15581.021	0.223	0.240	−0.50
13	36	*f*	15580.882	0.220	0.224	−0.12
13	37	*e*	15605.327	0.667	0.670	−0.03
13	37	*e*	15605.327	0.667	0.630	0.42
13	37	*f*	15605.190	0.659	0.650	0.10
13	38	*e*	15629.379	1.75	1.20	3.25
13	38	*f*	15629.245	1.73	1.60	0.59

TABLE IV. (*Continued*.)

v	J	p	$E_{v,J}(\mathrm{cm}^{-1})$	$\Gamma_{\mathrm{calc}}(\mathrm{cm}^{-1})$	$\Gamma_{\mathrm{obs}}(\mathrm{cm}^{-1})$	$\frac{\Gamma_{\mathrm{calc}}-\Gamma_{\mathrm{obs}}}{unc(\Gamma)}$
14	25	*e*	15444.220	0.014 9	0.030	−3.60
14	26	*f*	15462.030	0.041 8	0.059	−2.07
14	27	*e*	15480.318	0.115	0.124	−0.52
15	15	*e*	15399.571	0.120	0.136	−0.85
15	16	*e*	15409.932	0.214	0.172	1.77
15	16	*f*	15409.903	0.214	0.225	−0.35
15	17	*e*	15420.753	0.383	0.420	−0.64
15	17	*e*	15420.753	0.383	0.445	−0.99
15	17	*f*	15420.722	0.381	0.323	1.27
15	18	*f*	15431.956	0.673	0.60	0.85
15	19	*e*	15443.596	1.17	1.0	1.19
15	20	*f*	15455.496	1.96	1.9	0.23

[a]On this energy scale, the $B\,^1\Pi_u$ state asymptote lies at an energy of 14 903.983 468 cm^{-1} for $^{7,7}\mathrm{Li}_2$, and at 14 903.632 116 cm^{-1} for $^{6,6}\mathrm{Li}_2$.

difference cannot be definitively determined, but the large number of free parameters associated with the SPP analysis, in which each of the (in this case) 83 potential function values is a parameter in the fit, may have made it difficult to attain optimal convergence. Another source of differences may be the lack of high-order smoothness of SPP model potentials, which is discussed below.

The difference between the present analytical potential and the SPP function of Ref. 27 is shown by the solid curve in the upper segment (and inset) of Fig. 4, while the dotted curve there shows the 95% confidence limit uncertainty in our fitted DELR potential, as calculated using parameter uncertainties and the correlation matrix from the fit [see Eq. (7) of Ref. 57]. To place these results in context, the lower segment of this figure shows our recommended potential on the same (logarithmic) radial scale. The differences are clearly quite significant, especially outside the central data-sensitive region. It seems reasonable to attribute the oscillations in these differences to shortcomings of local cubic segments of the spline function defining the SPP potential, rather than to spurious oscillations of the fully analytic DELR function. However, the fact that the quality of fit to the $^{7,7}\mathrm{Li}_2$ f-parity data was only 36% worse for the SPP potential (see Table V) means that the net effect of these oscillating differences in the data-sensitive region is not excessive.

An unavoidable problem encountered whenever one uses a pointwise potential in dynamical calculations is ''interpolation noise,'' which we define as the uncertainty in our knowledge of a function due to dependence on the choice of interpolation method. Some interpolation noise will always be present when using a pointwise potential, while with a FAP function this problem simply does not arise. For example, an $\{N_S,N_L\}=\{9,9\}$ DELR potential function will be everywhere continuous and smooth to all orders, while the recommended $\{N_S,N_L\}=\{5,9\}$ DELR function is continuous and smooth to all orders everywhere except at the single point $r=r_e$, where derivatives of order $N_S+1=6$ and higher are discontinuous. In contrast, cubic spline interpolation through a given set of points (as in the SPP potential form) yields a function whose third derivative is discontinuous at *every internal spline mesh point* and for which all higher-order derivatives are identically zero. This lack of high-order smoothness is unphysical and is another possible

TABLE V. Quality of agreement with the f-parity data for $^{7,7}\mathrm{Li}_2$ obtained using the SPP potential of Ref. 27 and the present DELR potential model.

	No. data	SPP potential[a]	DELR fitted	Potential Table III
rmsr(frequencies)	663	1.318	0.965	1.030
rmsr(widths)	49	1.194	1.144	1.147
rmsr(total)	712	1.310	0.979	1.039

[a]Reference 27.

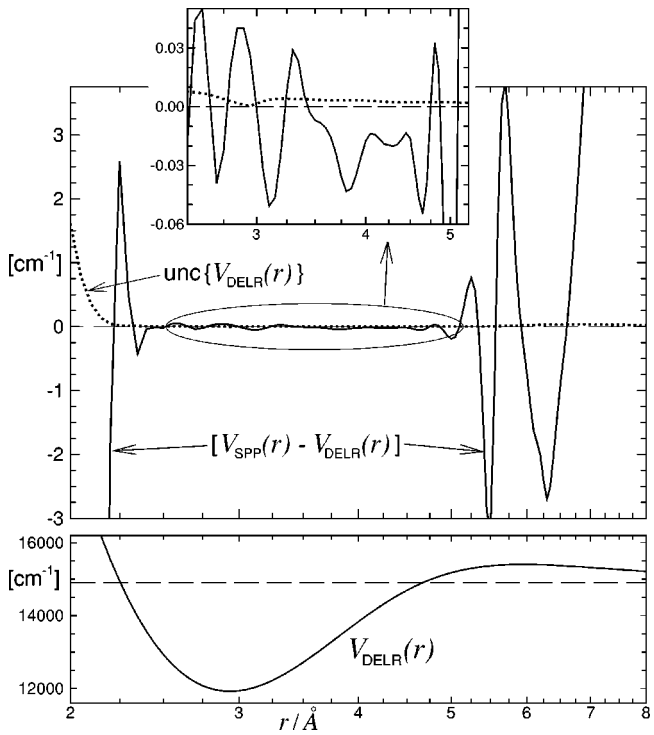

FIG. 4. Upper: differences between the present analytical DELR potential and the published SPP function for $B\,^1\Pi_u$-state Li_2 (solid curve) and 95% confidence limit uncertainties in our DELR potential (dotted curve). Lower: the present recommended DELR potential function.

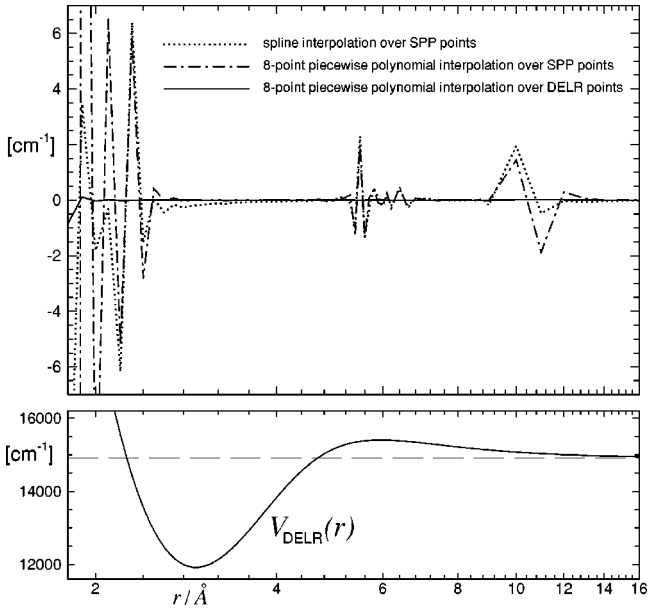

FIG. 5. Upper: Interpolation noise tests for the $^{7,7}Li_2(B\,^1\Pi_u)$ SPP function of Ref. 27 (dotted and dot-dashed plots) and for points generated from the present fully analytic DELR potential on the same mesh (solid curve). Lower: the present recommended DELR potential function.

source of the differences in quality of fit seen in Table V.

An indication of the magnitude of the interpolation noise associated with application of a given interpolation scheme to a particular set of data may be obtained in the following manner.[97] One by one, each of the data comprising an N-point set of function values is dropped from the data set, and the interpolation scheme applied to the remaining $N-1$ data to predict the value of the missing datum. The discrepancies between the interpolated values and the original function values they are supposed to represent provide a measure of the lack of smoothness in the given data array, and the different magnitudes of such discrepancies for different interpolation schemes indicate which scheme should be used in a given case. (This type of test should always be used to determine how to best interpolate over *ab initio* potential energy arrays for performing dynamical calculations.[97]) Figure 5 plots the discrepancies obtained on applying this interpolation test to the 83 points defining the SPP potential function of Ref. 27: The dotted lines join the discrepancies obtained using a cubic spline interpolation scheme, while the dash-dotted lines join those obtained on applying piecewise eight-point polynomial interpolation to that same data set. Quite large amplitude discrepancies occur at the inner and outer ends of the data-sensitive region (roughly 2.25–5.6 Å), which shows that the published SPP potential lacks smoothness there. In contrast, application of the same test to a set of 83 points generated from our analytic DELR function on the same radial mesh yields the discrepancies joined by solid line segments in the upper segment of Fig. 5. The fact that the latter are essentially zero on the scale of this plot attests to the much greater degree of smoothness of an FAP potential such as our DELR function.

E. Comparison with a conventional "parameter-fit" analysis

The most widely used approach for spectroscopic data reduction involves representing the level energies connected by the observed transitions with sets of "molecular constants."[34] Those constants are usually either a set of "band constants" $\{K_m^{(\alpha)}(v)\}=\{G_v^{(\alpha)},B_v^{(\alpha)},-D_v^{(\alpha)},H_v^{(\alpha)},\ldots,\text{etc.}\}$ for each vibrational level of each isotopomer α, or coefficients of expansions in which the vibrational and isotopomer dependence of each type of band constant is represented by a mass-scaled power series expansion in terms of a set of Dunham constants for the chosen reference isotopomer, $\alpha=1$,

$$K_m^{(\alpha)}(v)=\sum_l Y_{l,m}^{(1)}(\mu_1/\mu_\alpha)^{m+l/2}(v+\tfrac{1}{2})^l. \tag{37}$$

Straightforward generalization of these expression may incorporate BOB corrections, as required,[32] and analogous empirical band-constant or Dunham-expansion-type representations are used to represent Λ-doubling splittings. As this "parameter-fit" approach is still the most common way of rationalizing diatomic molecule data sets, it seems useful to compare it with the DPF approach presented above.

As a preliminary step in their analysis of this system, Bouloufa *et al.*[27] presented the results of a conventional band-constant fit to their full $^{7,7}Li_2$ data set. While they did obtain a good fit, it required some 112 conventional band constants $\{K_m(v)\}$ and 34 Λ-doubling band constants $\{q_m(v)\}$. Although the associated fits were very highly correlated, we found that a good fit can in fact be obtained using some 82 Dunham $\{Y_{l,m}\}$ parameters and 7 Dunham-type Λ-doubling expansion parameters [the resulting $Y_{l,m}$ expansions had orders {14, 14, 13, 11, 9, 7, 5, 2} for $m=0-7$, respectively, while the $q_{l,m}$ expansions required $(v+\frac{1}{2})$ polynomials of order 4 and 3 for $m=1$ and 2, respectively]. However, while this is 40% fewer parameters than were required by the band-constant analysis, it is still more than a factor of 6 larger than the 14 (11 potential function and 3 Λ-doubling) parameters required by our DPF analysis of the $^{7,7}Li_2$ data. It might be argued that this comparison is not really fair, since it is well known that centrifugal distortion constants (CDC's), and hence all $Y_{l,m}$ parameters for $m\geqslant 2$ are implicitly determined by the vibrational energy and inertial rotation constant ($m=0$ and 1) expansions, and hence could be held fixed at calculated values[98] in a self-consistent constrained-CDC analysis.[99–102] However, even if the 29 $m=0$ and 1 Dunham expansion parameters were the only ones which had to be determined by the fit, that would still be almost three times as many fitting parameters as are required to define our DELR potential function.

It is interesting to note that the success of the present analysis, which requires only three fitted parameters to accurately describe the Λ-doubling splittings, indicates that conventional Λ-doubling $\{q_m^{(\alpha)}(v)\}$ or $\{q_{l,m}^{(1)}\}$ coefficients for $m>1$ are implicitly determined by those for $m=1$. In particular, if the three quadratic $(m=2)$ $q_{l,m}^{(\alpha)}$ coefficients are omitted from the Dunham-type analysis described above, the value of rmsr more than doubles, and this cannot be compen-

TABLE VI. Leading Dunham coefficients and complete set of Λ-doubling expansion parameters for $B\,^1\Pi_u$ state Li_2 obtained from a combined-isotopomer fit to all 3153 transition frequencies for the three isotopomers; numbers in parentheses are 95% confidence limit uncertainties (Ref. 94).

		From all-isotopomer fit $^7Li\,^7Li$	Mass scaling $^7Li\,^6Li$	Adding BOB corrections $^6Li\,^6Li$
	$Y_{1,0}$	271.81351(55000)	282.8908582	293.549925
	$Y_{2,0}$	−4.81(87)	−5.20987178	−5.6096965
	$Y_{3,0}$	1.569(730)	1.768807809	1.976441249
	$Y_{0,1}$	0.556909(290)	0.602989896	0.649032031
	$Y_{1,1}$	−0.005817(1200)	−0.006145144	−0.0064054185
	$Y_{2,1}$	−0.0045(20)	−0.00547515513	−0.00657489066
10^4	$q_{0,1}$	1.94(3)	2.27623	2.63932
10^4	$q_{1,1}$	−0.051(9)	−0.062279	−0.074935
10^4	$q_{2,1}$	0.0064(10)	0.008134	0.0101558
10^4	$q_{3,1}$	−0.000409(37)	−0.000541	−0.00070094
10^8	$q_{0,2}$	−1.19(12)	−1.6382	−2.2026
10^8	$q_{1,2}$	0.02(3)	0.02866	0.03998
10^8	$q_{2,2}$	−0.0091(19)	−0.01357	−0.019646

sated for by increasing the order of the $m=1$ $\{q_{l,m}^{(\alpha)}\}$ polynomial. In contrast, the present perturbation potential treatment of Λ doubling is based on only a single radial function which is linearly proportional to $[J(J+1)]$.[103]

On extending the above comparisons to combined-isotopomer fits and allowing for BOB correction terms in the level energy expressions,[32] we were also able to achieve a good fit (rmsr=0.789) to all of the 3153 transition frequency data for the three isotopomers. However, in addition to the 82 $\{Y_{l,m}^{(1)}\}$ and 7 $\{q_{l,m}^{(1)}\}$ coefficients, this required some 40 empirical $\{\delta_{l,m}^{\mathrm{Li}}\}$ correction parameters, a startling increase over the *two* fitted BOB potential correction function parameters required by the present DPF analysis. This huge difference reflects the fact that in a potential-fit analysis the BOB correction function only needs to account for the difference between the effective potential energy functions for the different isotopomers, while in a parameter-fit analysis it must also account for the breakdown of the first-order semiclassical quantization condition on which the reduced-mass scaling of Eq. (37) is based. Note too that the fact that rmsr for this Dunham-type fit is slightly (ca. 9%) smaller than that associated with our DFP fit is not physically significant. Such artificial apparent improvements in quality of fit are expected when the centrifugal distortion constants are treated as free parameters in the fit instead of being required to be "mechanically consistent" with the potential function defined by the vibrational energies and inertial rotational constants. In summary, it is clear that conventional level-energy parameter fits are in all regards a much less compact and effective way to represent these data and their isotopomer dependence than is a DPF analysis.

In spite of the above, spectroscopists' enduring affection for using Dunham-type parameters to characterize molecules leads us to report some of the leading coefficients of our comprehensive Dunham-type fit in Table VI. Note that the constants for the minor isotopomers incorporate both the reduced-mass scaling of Eq. (37) and the effect of Dunham-type BOB correction coefficients $\{\delta_{l,m}^{\mathrm{Li}}\}$, as discussed in Ref. 32. Note too that the reduced-mass dependence of the Dunham-type Λ-doubling coefficients

$$q_m^{(\alpha)}(v)=\sum_l q_{l,m}^{(1)}(\mu_1/\mu_\alpha)^{2m+l/2}(v+\tfrac{1}{2})^l \tag{38}$$

differs from that for normal Dunham coefficients $Y_{l,m}^{(\alpha)}$ seen in Eq. (37). A complete listing of the Dunham-type vibration–rotation, Λ-doubling, and BOB expansion coefficients obtained in this fit are included with the supplementary data supplied to this journal's electronic data archive.[94]

V. CONCLUSIONS

The directly-fitted DELR potential energy function of Table III is the most accurate potential for $B\,^1\Pi_u$ state of Li_2 reported to date, reproducing all available multiple-isotopomer transition frequency and tunneling predissociation data (on average) to within the experimental uncertainties, in a fully quantum-mechanical analysis. For the reduced data set used in Ref. 27 the present model gives distinctly better agreement with experiment, and the analytic form of the DELR potential function makes it much easier to use than the pointwise SPP potential reported therein. The present analysis is also the first combined-isotopomer DPF analysis reported for Li_2, and it yields the first "adiabatic" atomic-mass-dependent BOB potential energy correction function reported for this molecule. This function indicates that for $^{6,6}Li_2$ the well depth $\mathcal{D}_e(B)$ is $0.102(\pm 0.018)$ cm^{-1} deeper, the barrier height $0.048(\pm 0.008)$ cm^{-1} higher than the corresponding quantities for $^{7,7}Li_2$. To our knowledge, this is the first quantitative determination of such isotopomer differences for any state of Li_2.

The results of Sec. IV E dramatically illustrate the fact that while parameter-fit analyses can work for challenging data sets such as that encountered here, they may require up to an order of magnitude more parameters to yield an equivalent quality of fit (140 versus 14). Moreover, polynomial level-energy expressions are notoriously unreliable for extrapolation, while the model potential energy and coupling functions determined here should yield quite reliable predictions for virtually all unobserved levels of this system.

Another noteworthy result here is the success of our perturbation-potential function treatment of Λ-doubling splittings. While neglect of Λ doubling increased the rms error of the fit by more than a factor of 20 and some 7 Dunham-type constants (or 34 band-constant terms for the $^{7,7}Li_2$ data alone) are required to adequately represent this behavior in a conventional parameter-fit analysis, the present work shows that a slowly varying a radial strength function defined by only three empirical parameters fully represents this behavior in a DPF analysis. This is certainly not the first time the effect of Λ doubling has been interpreted in terms of a radial perturbation function,[104] but it is one of the first in which such a treatment has been incorporated in a combined-isotopomer DPF data analysis, and the fact that this radial correction function treatment obviates the need for a quadratic-in-$[J(J+1)]$ splitting term attests to its validity. It is also interesting to see that the present treatment of Λ dou-

bling can provide an effective empirical method for determining the symmetry of the dominant state(s) giving rise to the splittings.

The success of the present analysis also attests to the utility of the DELR potential energy function model. Requiring only 11 parameters to be determined by the fit, it provides a much more compact and portable representation of the potential function for this system than does the set of 83 turning point energies which define the SPP potential function of Ref. 27. Moreover, our {5,9} DELR function is continuous and smooth to all orders everywhere except at the one point $r=r_e$ where its sixth- and higher-order derivatives are discontinuous; this makes it smoother and better behaved than the cubic spline SPP function. These considerations, together with the interpolation noise test illustrated by Fig. 5, indicate that whenever possible a fully analytic ("FAP") potential such as the DELR function introduced here (or the MLJ or GMO functions mentioned earlier) should be preferred to pointwise model potential such as the SPP function.

In spite of the above conclusion, it is important to recognize that the SPP potential form introduced by Pashov and co-workers has proved to provide a remarkably robust and effective way of treating a wide variety of problems.[27,36,58–61] A particular strength of that model is the fact that it has more local flexibility than do fully analytical potential function forms, in that a shift of one potential point has only a modest effect on the function outside its immediate neighborhood. This would tend to make the SPP model the method of choice for cases where the potential has substantial local structure or undergoes an abrupt change of character on a small fraction of the overall interval, such as occurs near an avoided curve crossing. In contrast, a change in one of the parameters defining a FAP potential such as our DELR function will in general affect the potential across the whole domain. This makes the parameters defining FAP potentials very highly correlated and can give rise to difficulty in achieving full unique convergence in a fit.

ACKNOWLEDGMENTS

We are pleased to express our gratitude to Dr. A. J. Ross for providing us with the experimental data used in this analysis, for many helpful discussions, and for insightful critical comments on the manuscript. This research has been supported by the Natural Sciences and Engineering Research Council of Canada.

[1] W. M. Kosman and J. Hinze, J. Mol. Spectrosc. **56**, 93 (1975).
[2] C. R. Vidal and H. Scheingraber, J. Mol. Spectrosc. **65**, 46 (1977).
[3] W. Weickenmeier, U. Deimer, M. Wahl, M. Raab, W. Demtröder, and W. Müller, J. Chem. Phys. **82**, 5354 (1985).
[4] J. A. Coxon, J. Mol. Spectrosc. **117**, 361 (1986).
[5] M. Gruebele, E. Keim, A. Stein, and R. J. Saykally, J. Mol. Spectrosc. **131**, 343 (1988).
[6] J. A. Coxon and P. G. Hajigeorgiou, J. Mol. Spectrosc. **150**, 1 (1991).
[7] R. Brühl, J. Kapetanakis, and D. Zimmermann, J. Chem. Phys. **94**, 5865 (1991).
[8] H. G. Hedderich, M. Dulick, and P. F. Bernath, J. Chem. Phys. **99**, 8363 (1993).
[9] J. A. Coxon and R. Colin, J. Mol. Spectrosc. **181**, 215 (1997).
[10] A. Šurkus, Chem. Phys. Lett. **279**, 236 (1997).
[11] E. G. Lee, J. Y. Seto, T. Hirao, P. F. Bernath, and R. J. Le Roy, J. Mol. Spectrosc. **194**, 197 (1999).
[12] J. Y. Seto, R. J. Le Roy, J. Vergès, and C. Amiot, J. Chem. Phys. **113**, 3067 (2000).
[13] J. A. Coxon, J. Mol. Spectrosc. **133**, 96 (1989).
[14] J. A. Coxon and J. F. Ogilvie, Can. J. Spec. **34**, 137 (1989).
[15] J. A. Coxon and P. G. Hajigeorgiou, J. Mol. Spectrosc. **139**, 84 (1990).
[16] J. A. Coxon and P. G. Hajigeorgiou, J. Mol. Spectrosc. **142**, 254 (1990).
[17] J. A. Coxon and P. G. Hajigeorgiou, J. Mol. Spectrosc. **193**, 306 (1999).
[18] J. A. Coxon and P. G. Hajigeorgiou, J. Mol. Spectrosc. **203**, 49 (2000).
[19] J. Y. Seto, Z. Morbi, F. Charron, S. K. Lee, P. F. Bernath, and R. J. Le Roy, J. Chem. Phys. **110**, 11 756 (1999).
[20] R. J. Le Roy and Y. Huang, J. Mol. Struct.: THEOCHEM **591**, 175 (2002).
[21] P. G. Hajigeorgiou and R. J. Le Roy, J. Chem. Phys. **112**, 3949 (2000).
[22] J. Y. Seto, M.Sc. thesis, Department of Chemistry, University of Waterloo, 2000.
[23] Y. Huang, M.Sc. thesis, Department of Chemistry, University of Waterloo, 2001.
[24] I. Russier, F. Martin, C. Linton, P. Crozet, A. J. Ross, R. Bacis, and S. Churassy, J. Mol. Spectrosc. **168**, 39 (1994).
[25] N. Bouloufa, P. Cacciani, R. Vetter, and A. Yiannopoulou, J. Chem. Phys. **111**, 1926 (1999).
[26] M. M. Hessel and C. R. Vidal, J. Chem. Phys. **70**, 4439 (1979).
[27] N. Bouloufa, P. Cacciani, R. Vetter, A. Yiannopoulou, F. Martin, and A. J. Ross, J. Chem. Phys. **114**, 8445 (2001).
[28] F. Martin and A. J. Ross (private communication).
[29] J. K. G. Watson, J. Mol. Spectrosc. **80**, 411 (1980).
[30] J. K. G. Watson, J. Mol. Spectrosc. (to be published).
[31] J. F. Ogilvie, J. Phys. B **27**, 47 (1994).
[32] R. J. Le Roy, J. Mol. Spectrosc. **194**, 189 (1999).
[33] The notation for BOB correction functions used here differs that of our earlier work (Refs. 20 and 32) in an effort to make it more consistent with that used by others (Refs. 29–31) and to avoid confusion with the "q" notation commonly used for Λ-doubling parameters. Note, however, that our use of the reference-isotopomer convention of Ref. 32 means that the present $\tilde{S}^A_{\rm ad}(r)$ differs from Watson's (Refs. 29 and 30) $\tilde{S}^A(r)$ by the factor $\Delta M_A^{(\alpha)}/m_e$ and that our $\tilde{R}^A_{\rm na}(r)$ differs from his $\tilde{R}^A(r)$ by the factor $M_A^{(1)}/m_e$, where m_e is the electron mass.
[34] G. Herzberg, *Spectra of Diatomic Molecules* (Van Nostrand, Toronto, 1950).
[35] H. Lefebvre-Brion and R. W. Field, *Perturbations in the Spectra of Diatomic Molecules* (Academic, New York, 1986).
[36] W. Jastrzębski, P. Kowalczyk, and A. Pashov, J. Mol. Spectrosc. **209**, 50 (2001).
[37] A. Unsöld, Z. Phys. **43**, 374 (1927); **43**, 563 (1927).
[38] P. Lindner and P.-O. Löwdin, Int. J. Quantum Chem., Symp. **2**, 161 (1968).
[39] P. F. Bernath, *Spectra of Atoms and Molecules* (Oxford University Press, Oxford, 1995).
[40] I. Schmidt-Mink, W. Müller, and W. Meyer, Chem. Phys. **92**, 263 (1985).
[41] Centrifugally distorted potentials for $J>0$ always have such barriers (except for ion pair states).
[42] R. J. Le Roy and R. B. Bernstein, J. Chem. Phys. **54**, 5114 (1971).
[43] R. J. Le Roy and W.-K. Liu, J. Chem. Phys. **69**, 3622 (1978).
[44] J. N. L. Connor and A. D. Smith, Mol. Phys. **43**, 397 (1981).
[45] *Handbook of Mathematical Functions*, edited by M. Abramowitz and I. A. Stegun (Dover, New York, 1970).
[46] J. W. Cooley, Math. Comput. **15**, 363 (1961).
[47] J. Cashion, J. Chem. Phys. **39**, 1872 (1963).
[48] R. J. Le Roy, "LEVEL 7.5: A Computer Program for Solving the Radial Schrödinger Equation for Bound and Quasibound Levels," University of Waterloo Chemical Physics Research Report No. CP-655, 2002. The source code and manual for this program may be obtained from the "Computer Programs" link at http://leroy.uwaterloo.ca
[49] (a) G. Gamow, Z. Phys. **51**, 204 (1928); (b) R. W. Gurney and E. U. Condon, Phys. Rev. **33**, 127 (1929).
[50] R. L. Liboff, *Introductory Quantum Mechanics* (Addison-Wesley, Reading, MA, 1992).
[51] M. S. Child, in *Molecular Spectroscopy*, edited by R. Barrow, D. A. Long, and D. J. Millen (Chemical Society of London, London, 1974), Vol. 2, Specialist Periodical Report 7, pp. 466–512.
[52] M. G. Barwell, R. J. Le Roy, P. Pajunen, and M. S. Child, J. Chem. Phys. **71**, 2618 (1979).
[53] P. Pajunen, J. Chem. Phys. **73**, 6232 (1980).
[54] P. Pajunen, Ph.D. thesis, Oxford University, 1978.

[55] R. J. Le Roy, in *Semiclassical Methods in Molecular Scattering and Spectroscopy*, edited by M. Child, Vol. 53 of Series C—Mathematical and Physical Sciences (Reidel, Dordrecht, 1980), pp. 109–126.
[56] R. J. Le Roy, J. Y. Seto, and Y. Huang, computer code DSPOTFIT (Diatomic Singlet Potential Fits), will be available from http://leroy.uwaterloo.ca in the near future.
[57] R. J. Le Roy, J. Mol. Spectrosc. **191**, 223 (1998).
[58] A. Pashov, W. Jastrzębski, and P. Kowalczyk, Comput. Phys. Commun. **128**, 622 (2000).
[59] A. Pashov, W. Jastrzębski, and P. Kowalczyk, J. Chem. Phys. **113**, 6624 (2000).
[60] A. Pashov, W. Jastrzębski, W. Jaśniecki, V. Bednarska, and P. Kowalczyk, J. Mol. Spectrosc. **203**, 264 (2000).
[61] F. Martin, P. Crozet, A. J. Ross, M. Aubert-Frécon, P. Kowalczyk, W. Jastrzębski, and A. Pashov, J. Chem. Phys. **115**, 4118 (2001).
[62] A. Grochola, W. Jastrzebski, P. Kowalczyk, P. Crozet, and A. J. Ross, Chem. Phys. Lett. **372**, 173 (2003).
[63] J. L. Dunham, Phys. Rev. **41**, 713 (1932); **41**, 721 (1932).
[64] G. Simons, R. G. Parr, and J. M. Finlan, J. Chem. Phys. **59**, 3229 (1973).
[65] A. J. Thakkar, J. Chem. Phys. **62**, 1693 (1975).
[66] J. F. Ogilvie, Proc. R. Soc. London, Ser. A **378**, 287 (1981).
[67] A. A. Surkus, R. J. Rakauskas, and A. B. Bolotin, Chem. Phys. Lett. **105**, 291 (1984).
[68] J. Tellinghuisen, J. Mol. Spectrosc. **173**, 223 (1995).
[69] H. Margenau, Rev. Mod. Phys. **11**, 1 (1939).
[70] J. O. Hirschfelder, C. F. Curtiss, and R. B. Bird, *Molecular Theory of Gases and Liquids* (Wiley, New York, 1964).
[71] R. J. Le Roy, in *Molecular Spectroscopy*, edited by R. Barrow, D. A. Long, and D. J. Millen (Chemical Society of London, London, 1973), Vol. 1, Specialist Periodical Report 3, pp. 113–176.
[72] H. Kreek and W. J. Meath, J. Chem. Phys. **50**, 2289 (1969).
[73] H. Kreek, Y. H. Pan, and W. J. Meath, Mol. Phys. **19**, 513 (1970).
[74] Y. H. Pan and W. J. Meath, Mol. Phys. **20**, 873 (1971).
[75] C. Douketis, G. Scoles, S. Marchetti, M. Zen, and A. J. Thakkar, J. Chem. Phys. **76**, 3057 (1982).
[76] C. Douketis, J. M. Hutson, B. J. Orr, and G. Scoles, Mol. Phys. **52**, 763 (1984).
[77] In particular, for a pair of identical atoms X, $\rho_d = \rho_d(X) = (I_X/I_H)^{2/3}$, where I_X is the ionization energy of atom X and I_H that for a ground-state H atom, and for a pair of unlike atoms X and Y, $\rho_d(X,Y) = 2\rho_d(X)\rho_d(X)/[\rho_d(X)+\rho_d(X)]$.
[78] A. Koide, W. J. Meath, and A. R. Allnatt, Chem. Phys. **58**, 105 (1981).
[79] K. T. Tang and J. P. Toennies, J. Chem. Phys. **80**, 3726 (1984).
[80] D. K. Watson, C. J. Cerjans, S. Guberman, and A. Dalgarno, Chem. Phys. Lett. **50**, 181 (1977).
[81] H.-K. Chung, K. Kirby, and J. F. Babb, Phys. Rev. A **60**, 2002 (1999).
[82] D. D. Konowalow and J. L. Fish, Chem. Phys. **84**, 463 (1984).
[83] D. D. Konowalow and J. L. Fish, Chem. Phys. **77**, 435 (1983).
[84] R. Poteau and F. Spiegelmann, J. Mol. Spectrosc. **171**, 299 (1995).
[85] (a) K. Wurm, Naturwissenschaften **48**, 1028 (1928); (b) Z. Phys. **58**, 562 (1929); (c) **59**, 35 (1929).
[86] A. Harvey and F. A. Jenkins, Phys. Rev. **35**, 789 (1930).
[87] R. A. Bernheim, L. P. Gold, P. B. Kelly, C. Tomczyk, and D. K. Veirs, J. Chem. Phys. **74**, 3249 (1981).
[88] L. Li, G. Lazarov, and A. M. Lyyra, J. Mol. Spectrosc. **191**, 387 (1998).
[89] V. S. Ivanov, V. B. Sovkov, L. Li, A. M. Lyyra, G. Lazarov, and J. Huennekens, J. Mol. Spectrosc. **194**, 147 (1999).
[90] We are grateful to Dr. A. J. Ross for providing us with the converted $^{7,7}Li_2$ data set used in the analysis of Ref. 27.
[91] C. Linton, F. Martin, R. Bacis, and J. Vergès, J. Mol. Spectrosc. **142**, 340 (1990).
[92] C. J. Sansonetti, B. Richou, R. Engleman, Jr., and L. J. Radziemski, Phys. Rev. A **52**, 2682 (1995).
[93] The tunneling predissociation widths for $^{6,6}Li_2$ used here were refined values extracted from the data of Ref. 24 by A. J. Ross, to whom we are indebted for providing us with these results.
[94] See EPAPS Document No. E-JCPSA6-119-013338 for ASCII files containing listings of the data used in the present work and the complete parameter set yielded by the global Dunham-type analysis described in Sec. IV E. A direct link to this document may be found in the online article's HTML reference section. The document may also be reached via the EPAPS homepage (http://www.aip.org/pubservs/epaps.html) or from ftp.aip.org in the directory /epaps/. See the EPAPS homepage for more information.
[95] P. Cacciani and V. Kokoouline, Phys. Rev. Lett. **84**, 5296 (2000).
[96] N. Bouloufa, P. Cacciani, V. Kokoouline, F. Masnou-Seeuws, and L. Li, Phys. Rev. A **63**, 042507 (2001).
[97] R. J. Le Roy and R. B. Bernstein, J. Chem. Phys. **49**, 4312 (1968).
[98] (a) J. M. Hutson, J. Phys. B **14**, 851 (1981); (b) QCPE Bulletin, Vol. 2, No. 2, Program No. 435, Quantum Chemistry Program Exchange, Indiana University, Bloomington, Indiana.
[99] J. D. Brown, G. Burns, and R. J. Le Roy, Can. J. Phys. **51**, 1664 (1973).
[100] J. M. Hutson, S. Gerstenkorn, P. Luc, and J. Sinzelle, J. Mol. Spectrosc. **96**, 266 (1982).
[101] J. W. Tromp and R. J. Le Roy, J. Mol. Spectrosc. **109**, 352 (1985).
[102] Y. Liu, J. Li, D. Chen, L. Li, K. M. Jones, B. Ji, and R. J. Le Roy, J. Chem. Phys. **111**, 3494 (1999).
[103] Indeed, the parallel manner in which the $\Delta V_\Lambda^{(\alpha)}(r)$ and centrifugal potential terms contribute to Eq. (9) indicates that "mechanically consistent" higher-order $(m>1)$ $q_m^{(\alpha)}(v)$ Λ-doubling parameters may be generated in the same manner commonly used for calculating conventional centrifugal distortion constants (Ref. 100).
[104] J. A. Coxon and S. C. Foster, J. Mol. Spectrosc. **91**, 243 (1982).

Erratum: "Potential energy, Λ doubling and Born–Oppenheimer breakdown functions for the $B\,^1\Pi_u$ 'barrier' state of Li_2" [J. Chem. Phys. 119, 7398 (2003)]

Yiye Huang and Robert J. Le Roy[a)]
Guelph-Waterloo Centre for Graduate Work in Chemistry and Biochemistry, University of Waterloo, Waterloo, Ontario, Canada N2L 3G1

(Received 15 March 2007; accepted 15 March 2007; published online 27 April 2007)

[DOI: 10.1063/1.2723739]

While the coding and calculations for this paper were correct, two of the equations defining our expression for the vibrational period contain typographical errors. In particular, Eq. (15) contains a spurious negative sign, and should read

$$t_{\mathrm{vib}}^{\mathrm{un}}(E_{v,J}) = t_{\mathrm{vib}}^{\mathrm{cl}}(E_{v,J}) - \frac{\hbar}{2\pi}\left[\ln\{\varepsilon(E_{v,J})/2\pi\} + 2\pi\frac{d\arg\Gamma\left(\frac{1}{2} - i\varepsilon(E_{v,J})/2\pi\right)}{d\varepsilon(E_{v,J})}\right]\frac{\partial\varepsilon(E_{v,J})}{\partial E_{v,J}} \tag{15}$$

and Eq. (16) is missing an overall factor of $-1/(2\pi)$, and should read

$$\frac{d\arg\Gamma\left(\frac{1}{2} - i\varepsilon(E_{v,J})/2\pi\right)}{d\varepsilon(E_{v,J})} = -\frac{1}{2\pi}\left\{\Psi\left(\tfrac{1}{2}\right) + \sum_{k=0}\left[\frac{\left(k+\frac{1}{2}\right)^3}{[\varepsilon(E_{v,J})/2\pi]^2} + \left(k+\frac{1}{2}\right)\right]^{-1}\right\}. \tag{16}$$

We are grateful to Professor Stephen Ross for bringing these errors to our attention.

In addition, there was a power missing in the definition of the Λ-doubling radial strength function, and Eq. (36) should read

$$f_\Lambda(r) = \sum_{i=0} l_i y_{\mathrm{p}}(r)^i. \tag{36}$$

Finally, the recommended potential function defined by the parameters in Table III was based on damping functions with the form of Eq. (31), but with the numerical factors in the exponent having the *un*rounded values of 3.968 424 881 (rather than 3.97) and 0.389 246 07 (rather than 0.39). An updated set of potential function parameters obtained using damping functions based on the published data form (with 3.97 and 0.39) may be obtained from the authors.

[a)]Electronic mail: leroy@uwaterloo.ca

